JRC Scientific and Technical Reports

JRC Ispra EMEP – GAW regional station for atmospheric research

2009 report

Niels R. Jensen, Carsten Gruening, Mariana Adam, Fabrizia Cavalli, Paolo Cavalli, Fabrizio Grassi*, Alessandro Dell'Acqua, Sebastiao Martins Dos Santos, David Roux, Jean-Philippe Putaud

Climate Change Unit, Institute for Environment and Sustainability, JRC-Ispra, Italy.

*NOS s.r.l., Rome, Italy.

EUR 24678 EN - 2010

JRC EUROPEAN COMMISSION

ies Institute for Environment and Sustainability

The mission of the JRC-IES is to provide scientific-technical support to the European Union's policies for the protection and sustainable development of the European and global environment.

European Commission
Joint Research Centre
Institute for Environment and Sustainability

Contact information

J.-P. Putaud
IES-CCU, JRC, TP 050,
Via E. Fermi 2749
I-21027 Ispra (VA), Italy

E-mail: jean.putaud@jrc.ec.europa.eu
Tel.: +39-0332-785041
Fax: +39-0332-785022

http://ccu.jrc.ec.europa.eu/
http://ies.jrc.ec.europa.eu/
http://www.jrc.ec.europa.eu/

Niels R. Jensen
IES-CCU, JRC, TP 050,
Via E. Fermi 2749
I-21027 Ispra (VA), Italy

E-mail: niels.jensen@jrc.ec.europa.eu
Tel.: +39-0332-789225
Fax: +39-0332-785022

http://ccu.jrc.ec.europa.eu/
http://ies.jrc.ec.europa.eu/
http://ec.europa.eu/dgs/jrc/index.cfm
http://ec.europa.eu/index_en.htm

JRC 62602

EUR 24678 EN

ISSN 1018-5593

ISBN 978-92-79-18978-4

doi:10.2788/97714

Luxembourg: Publications Office of the European Union

Printed in Italy

JRC Ispra EMEP – GAW regional station for atmospheric research

2009 report

Niels R. Jensen, Carsten Gruening, Mariana Adam, Fabrizia Cavalli, Paolo Cavalli, Fabrizio Grassi*, Alessandro Dell'Acqua, Sebastiao Martins Dos Santos, David Roux, Jean-Philippe Putaud

Climate Change Unit, Institute for Environment and Sustainability, JRC-Ispra, Italy.
*NOS s.r.l., Rome, Italy.

EUR 24678 EN – 2010

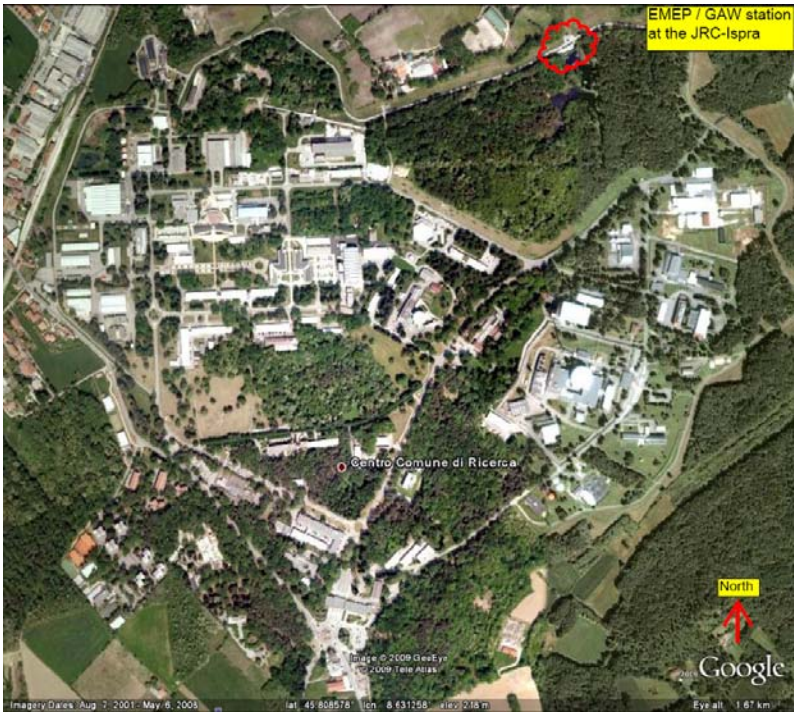

Fig. 1. JRC-Ispra site and the location of the EMEP-GAW station (red circle).

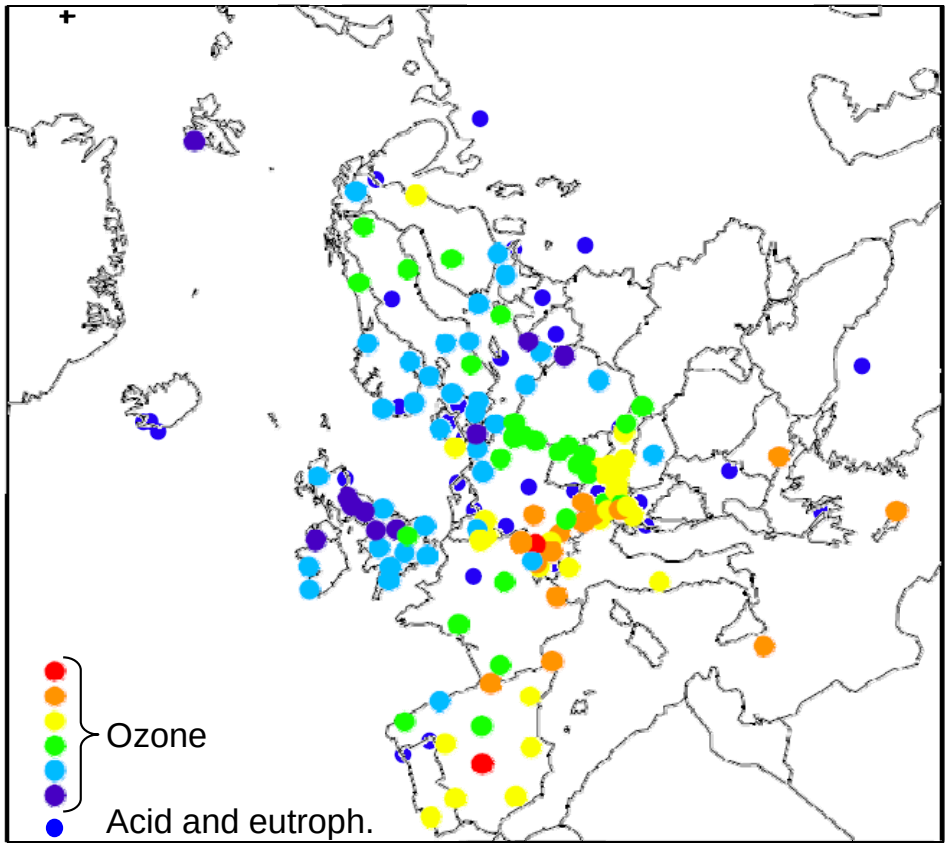

Fig. 2: EMEP stations reporting ozone, acidifying and eutrophying data in 2005.

Introduction

Location

The JRC station for atmospheric research (45°48.881'N, 8°38.165'E, 209 m a.s.l.) is located by the Northern fence of the JRC-Ispra site (see Fig. 1), situated in a semi-rural area at the NW edge of the Po valley in Italy. The station is several tens of km away from large emission sources like intense road traffic or big factories. The main cities around are Varese, 20 km east, Novara, 40 km south, Gallarate - Busto Arsizio, about 20 km south-east and the Milan conurbation, 60 km to the south-east. Busy roads and highways link these urban centers. Four industrial large source points (CO emissions > 1000 tons / yr) are located between 20 and 50 km E to SE of Ispra. The closest (20 km SSE) emits also > 2000 tons of NO_x per year (EMEP emission inventory 2000).

Mission

The aim of the JRC-Ispra EMEP-GAW station is to monitor the concentration of pollutants in the gas phase, the particulate phase and precipitations, as well as aerosol optical parameters, which can be used for assessing the impact of European policies on air pollution and climate change. Measurements are performed in the framework of international monitoring programs like the *Co-operative program for monitoring and evaluation of the long range transmission of air pollutants in Europe (EMEP)* of the UN-ECE *Convention on Long-Range Transboundary Air Pollution (CLRTAP)* and the *Global Atmosphere Watch (GAW)* program of the World Meteorological Organization (WMO).

The EMEP program (*http://www.emep.int/*)

Currently, 50 countries and the European Community have ratified the CLRTAP. Lists of participating institutions and monitoring stations (Fig. 2) can be found at: *http://www.nilu.no/projects/ccc/network/index.html*

The set-up and running of the JRC-Ispra EMEP station resulted from a proposal of the Directorate General for Environment of the European Commission in Brussels, in agreement with the Joint Research Centre, following the Council Resolution N° 81/462/EEC, article 9, of supporting the implementation of the EMEP programme.

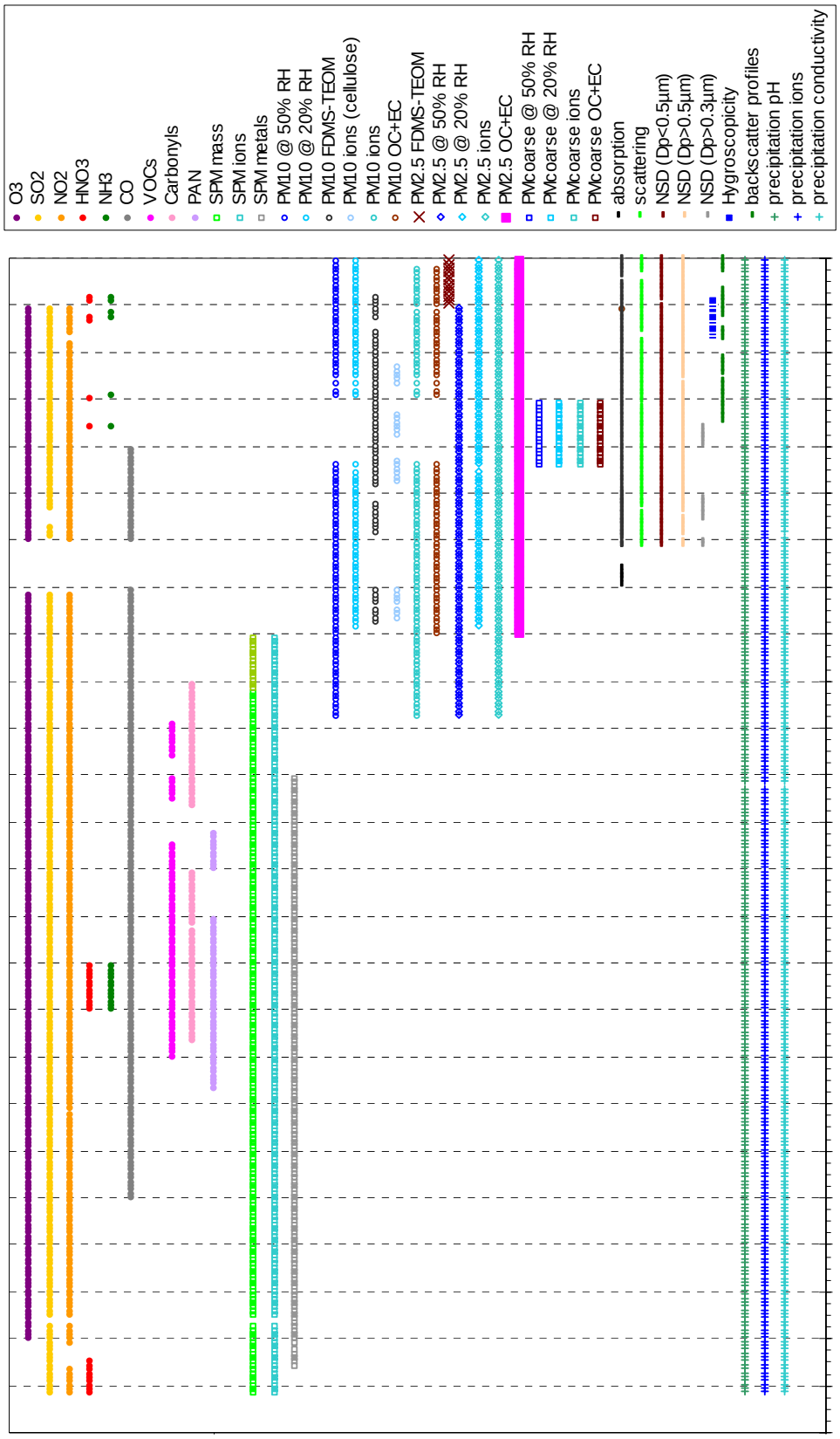

Fig. 3. Measurements performed at the JRC-Ispra station for atmospheric research since 1985.

Sources : This report, Gruening et al., 2009, Rembges et. al., 2003.

The JRC-Ispra station operates on a regular basis in the extended EMEP measurement program since November 1985. Data are transmitted yearly to the EMEP

Chemical Coordinating Centre (CCC) for data control and statistical evaluation, and available from the EBAS data bank (*http://ebas.nilu.no/*).

The GAW program (*http://www.wmo.int/web/arep/gaw/gaw_home.html*)

WMO's Global Atmosphere Watch (GAW) system was established in 1989 with the scope of providing information on the physico-chemical composition of the atmosphere. These data provide a basis to improve our understanding of both atmospheric changes and atmosphere-biosphere interactions. GAW is one of WMO's most important contributions to the study of environmental issues, with about 80 member countries participating in GAW's measurement program. Since December 1999, the JRC-Ispra station is also part of the GAW coordinated network of regional stations. Aerosol data submitted to EMEP and GAW are available from the World Data Centre for Aerosol (WDCA).

The institutional program (*http://ccu.jrc.ec.europa.eu*)

The JRC-Ispra station has been managed by the Climate Change Unit of the Joint Research Centre's (JRC) Institute for Environment and Sustainability since February 2002. From then on, its monitoring program has been focused on air pollution and climate forcing of short-lived agents such as tropospheric ozone and aerosols. Concretely, more sensitive gas monitors were introduced, as well as a set of new measurements providing aerosol characteristics that are linked to its radiative forcing.

The site is also being used for research and development purposes, mainly focusing on organic carbon sampling artefacts. The data obtained in Ispra are used for the design of the EMEP monitoring strategy and the revision of the EMEP sampling and analytical procedure manual.

Measurement data obtained at the JRC-Ispra station within the EMEP program and other projects can be retrieved from the EBAS database (*http://ebas.nilu.no/*), selecting Ispra as the station of interest. Historical data can also be downloaded from the Climate Change Unit web page *http://ccu.jrc.ec.europa.eu/* by selecting "what we do" → "existing datasets" and then going to "Yearly / Monthly Averages at the Montelibretti and Ispra EMEP Stations".

Table 1. Parameters measured during 2009

METEOROLOGICAL PARAMETERS	Pressure, temperature, humidity, wind, solar radiation
GAS PHASE	SO_2, NO, NO_2, NO_X, O_3, CO (not in 2009, but restarted 2010)
PARTICULATE PHASE	For $PM_{2.5}$: PM mass and Cl^-, NO_3^-, SO_4^{2-}, $C_2O_4^{2-}$, Na^+, NH_4^+, K^+, Mg^{2+}, Ca^{2+}, OC, and EC For PM_{10}: PM mass and Cl^-, NO_3^-, SO_4^{2-}, $C_2O_4^{2-}$, Na^+, NH_4^+, K^+, Mg^{2+}, Ca^{2+}, OC, and EC Number size distribution (10 nm - 10 µm) Aerosol absorption, scattering and back-scattering coefficient altitude-resolved aerosol back-scattering LIDAR for altitude resolved aerosol backscattering profiles H-TDMA for hygroscopic growth factors of the aerosols
PRECIPITATION PHASE	Cl^-, NO_3^-, SO_4^{2-}, $C_2O_4^{2-}$, Na^+, NH_4^+, K^+, Mg^{2+}, Ca^{2+} pH, conductivity

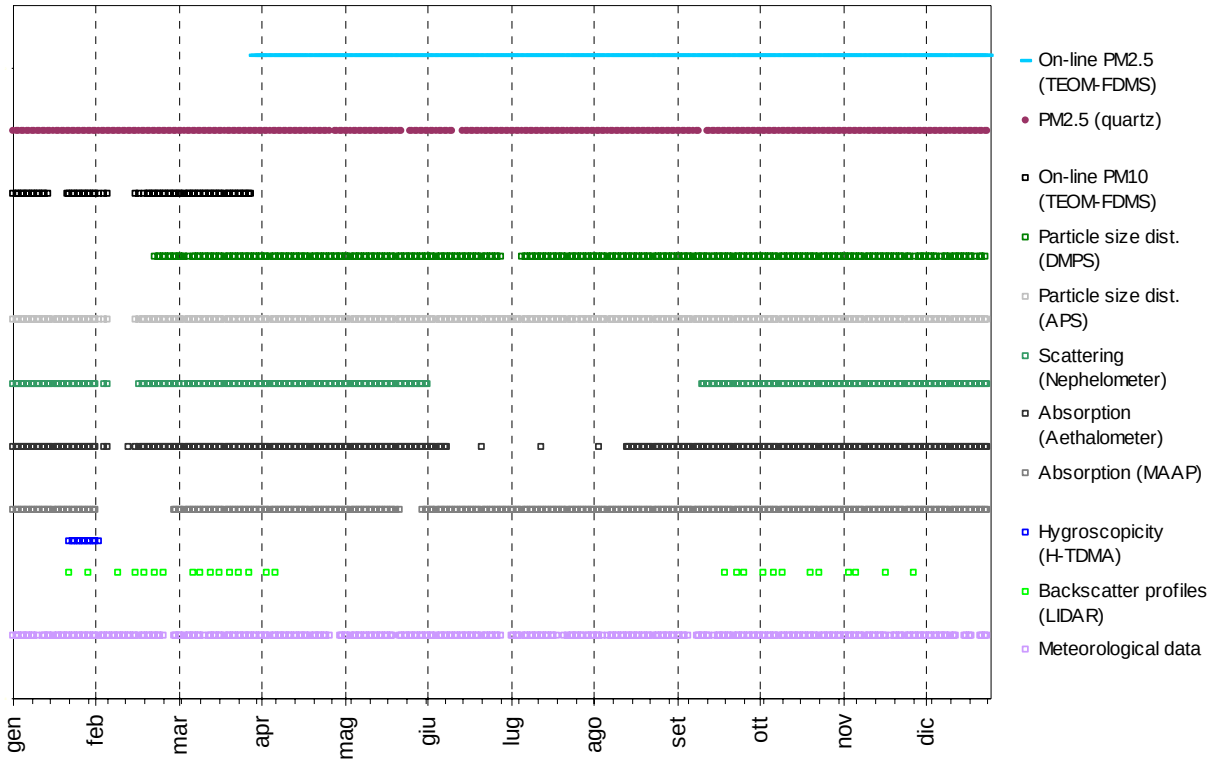

Fig. 4. The year 2009 data coverage at the JRC EMEP-GAW station.

Page left intentional blank

The JRC-Ispra station for atmospheric research monitoring program

Since 1985, the JRC-Ispra air monitoring station program evolved significantly (Fig. 3). The parameters measured at the JRC-Ispra station in 2009 are listed in Table 1. Fig. 4 shows the data coverage for 2009 (additional information about the JRC-Ispra air monitoring station and other stations from the EMEP network can also be found in the following papers: Van Dingenen et al., 2004; Putaud et al., 2004; Mira-Salama et al., 2008; Putaud et al., 2010).

Meteorological parameters were measured during the whole year 2009.

The gas phase species SO_2, NO_x, O_3 and CO were not measured during the year 2009, due to lack of man-power, but all of the gas phase measurements listed in Table 1 have been restarted in January 2010.

Particulate matter (PM2.5) samples were collected daily and analyzed for PM2.5 mass (at 20% RH), main ions, OC (organic carbon) and EC (elemental carbon). PM10 24-hour filter samples were normally collected four times a month on average and analyzed in the same way as the daily PM2.5 samples. On-line PM measurements (FDMS-TEOM, Filter Dynamics Measurement System - Tapered Element Oscillating Microbalance) were carried out from 01.01.2009 to 31.03.2009 for PM10 and PM2.5; thereafter it was PM2.5 and PM1.

Aerosol absorption coefficient and particle number size distribution (Dp < 600 nm) were measured continuously over the whole year. Particle number size distribution (Dp > 500 nm), and scattering coefficient were determined continuously as well.

The LIDAR (Laser Imaging Detection and Ranging) provided altitude resolved aerosol backscattering profiles during favourable weather conditions except for longer interruptions in April-July 2009 due to instrumental problems.

H-TDMA data were acquired during 2009 for the months of January and February while during 2008 the data were acquired during May, June, July, September, October and December. Since the H-TDMA results for 2008 were not reported during 2008 report (data were processed during early 2010) we show here the results for the entire period of the experiment (May 2008 – February 2009).

Precipitation was collected throughout the year and analyzed for pH, conductivity, and main ions.

Quality management

Quality management and the JRC-Ispra EMEP-GAW regional station

In May 2010 the JRC's Institute for Environment and Sustainability (which include the EMEP-GAW regional station) received the ISO 9001 certificate, so the year 2009 was also used to set-up a quality management system at the JRC-Ispra EMEP-GAW regional station. The "quality management system and EMEP-GAW regional station" include a server space at store1: \\Store1\emep\Quality_management where the following information can be found: List of instruments; information about calibrations, standards used and maintenance; standard operational procedures (SOP's); lifecycle sheets (e.g. log-books); manuals for the instruments, *etc*.

The measurement techniques

On-line Monitoring

Meteorological Parameters

Weather Transmitter:

Meteorological data and solar radiation were measured directly at the EMEP station with the instrumentation described below.

WXT510 (S/N: A1410009 & A1410011)

One WXT510 weather transmitter from Vaisala for the entire year and a second one from 23.06.2008 and onwards recorded simultaneously the six weather parameters temperature, pressure, relative humidity, precipitation and wind speed and direction.
The wind data measurements utilise three equally spaced ultrasonic transducers that determine the wind speed and direction from the time it takes for ultrasound to travel from one transducer to the two others. The precipitation is measured with a piezoelectrical sensor that detects the impact of individual raindrops and thus infers the accumulated rainfall. For the pressure, temperature and humidity measurements, separate sensors employing high precision RC oscillators are used.

CM11 (S/N: 058911) & CMP 11 (S/N: 070289)

To determine the solar radiation, a Kipp and Zonen CM11 was used. From 23.06.2008 and onwards an additional CMP11 Pyranometer have been installed that measure the irradiance (in W/m^2) on a plane surface from direct solar radiation and diffuse radiation incident from the hemisphere above the device. The measurement principle is based on a thermal detector. The radiant energy is absorbed by a black disc and the heat generated flows through a thermal resistance to a heat sink. The temperature difference across the thermal resistance is then converted into a voltage and precisely measured. Both the CM11 & CMP11 feature a fast response time of 12 s, a small non stability of +/-0.5 % and a small non linearity of +/-0.2 %.

Aerosol

PM10 mass concentration: Tapered Element Oscillating Mass balance, Series 1400a

Thermo FDMS – TEOM (S/N 140AB233870012 & 140AB253620409)

The Series 1400a TEOM® monitor incorporates an inertial balance patented by Rupprecht & Patashnick, now Thermo. It measures the mass collected on an exchangeable filter cartridge by monitoring the frequency changes of a tapered element. The sample flow passes through the filter, where particulate matter is collected, and then continues through the hollow tapered element on its way to an electronic flow control system and vacuum pump. As more mass collects on the exchangeable filter, the tube's natural frequency of oscillation decreases. A *direct* relationship exists between the tube's change in frequency and mass on the filter. The TEOM mass transducer does not require recalibration because it is designed and constructed from non-fatiguing materials. Calibration may be verified, however, using an optional Mass Calibration Verification Kit that contains a filter of known mass.
The instrument set-up includes a Sampling Equilibration System (SES) that allows a water strip-out without sample warm up by means of Nafion Dryers. In this way the air flow RH is reduced to < 30%, when TEOM® operates at 30 °C only. The Filter Dynamic Measurement System (FDMS) is based on measuring changes of the TEOM filter mass when sampling alternatively ambient and filtered air. The changes in the TEOM filter mass while sampling filtered air is attributed to sampling (positive or negative) artefacts, and is used to correct changes in the TEOM filter mass observed while sampling ambient air.

Particle number size distribution: Differential Mobility Particle Sizer (DMPS)

DMPS "B", CPC TSI 3010 (S/N 2051), CPC TSI 3772 (S/N 70847419)

The Differential Mobility Particle Sizer consists in a home-made medium size (28 cm) Vienna-type Differential Mobility Analyser (DMA) and a Condensation Particle Counter (CPC), TSI 3010 (S/N 2051) or TSI 3772 (S/N 70847419). Its setup follows the EUSAAR specifications for DMPS systems.
DMA's use the fact that electrically charged particles move in an electric field according to their electrical mobility. Electrical mobility depends mainly on particle size and electrical charge. Atmospheric particles are brought in the bipolar charge equilibrium in the bipolar diffusion charger (Eckert & Ziegler neutralizer with 370 MBq): a radioactive source (Kr-85) ionizes the surrounding atmosphere into positive and negative ions. Particles carrying a high charge can discharge by capturing ions of opposite polarity. After a very short time, particles reach a charged equilibrium such that the aerosol carries the bipolar Fuchs-Boltzman charge distribution. A computer program sets stepwise the voltage between the 2 DMA's electrodes (from 10 to 11500 V). Negatively charged particles are so selected according to their mobility. After a certain waiting time, the CPC measures the number concentration for each mobility bin. The result is a particle mobility distribution. The number size distribution is calculated from the mobility distribution by an inversion routine (from Stratmann and Wiedensohler, 1996) based on the bipolar charge distribution and the size dependent DMA transfer function. The CPC detection efficiency curve is not taken into account. The DMPS measured aerosol particles in the range 10 – 600 nm during an 8 minute cycle until 12.6.2009 and afterwards from 10 to 800 nm with a 10 minute cycle. It records data using 45 size channels for high-resolution size information. This submicrometer particle sizer is capable of measuring concentrations in the range from 1 to 2.4 x 10^6 particles/cm^3. Instrumental parameters that are necessary for data evaluation such as flow rates, relative humidity, ambient pressure and temperature are measured and saved as well
Accessories include:
- FUG High voltage cassette power supplies Series HCN7E – 12500 Volts.
- Rotary vacuum pump vane-type (sampling aerosol at 1 LPM)
- Controlled blower (circulating dry sheath air)

- Sheath air dryer only using silica gel until 27.10.2009, thereafter sheath and sample air dryer using Nafion; this mean that the DMPS started to sample in dry conditions from 27 October 2009 onwards.

- Mass flow meter and pressure transducer (to measure sheath air and sample flows).

Particle number size distribution: Aerodynamic Particle Sizer

APS TSI 3321 (S/N 70535014)

The APS 3321 is a time-of-flight spectrometer that measures the velocity of particles in an accelerating air flow through a nozzle.
Ambient air is sampled at 1 L/min, sheath air (from the room) at 4 L/min. In the instrument, particles are confined to the center-line of an accelerating flow by sheath air. They then pass through two broadly focused laser beams, scattering light as they do so. Side-scattered light is collected by an elliptical mirror that focuses the collected light onto a solid-state photodetector, which converts the light pulses to electrical pulses. By electronically timing between the peaks of the pulses, the velocity can be calculated for each individual particle.
Velocity information is stored in 1024 time-of-flight bins. Using a polystyrene latex (PSL) sphere calibration, which is stored in non-volatile memory, the APS Model 3321 converts each time-of-flight measurement to an aerodynamic particle diameter. For convenience, this particle size is binned into 52 channels (on a logarithmic scale).
The particle range spanned by the APS is from 0.5 to 20 µm in both aerodynamic size and light-scattering signal. Particles are also detected in the 0.3 to 0.5 µm range using light-scattering alone, and are binned together in one channel. The APS is also capable of storing correlated light-scattering-signal. *dN/dLogDp* data are averaged over 10 min.

Particle scattering and back-scattering coefficient

Nephelometer TSI 3563 (S/N 1081)

The integrating nephelometer is a high-sensitivity device capable of measuring the scattering properties of aerosol particles. The nephelometer measures the light scattered by the aerosol and then subtracting light scattered by the walls of the measurement chamber, light scattered by the gas, and electronic noise inherent in the detectors.
Ambient air is sampled at 20 L/min - until 18.11.2009 – and at 5.3 L/min afterwards from a whole air inlet (TSP). In addition, the Nephelometer started to sample in dry conditions from 18th of November 2009 onwards.
The three-color detection version of TSI nephelometer detects scattered light intensity at three wavelengths (450, 550, and 700 nm). Normally the scattered light is integrated over an angular range of 7–170° from the forward direction, but with the addition of the backscatter shutter feature to the Nephelometer, this range can be adjusted to either 7–170° or 90–170° to give total scatter and backscatter signals. A 75 Watt quartz-halogen white lamp, with a built-in elliptical reflector, provides illumination for the aerosol. The reflector focuses the light onto one end of an optical pipe where the light is carried into the internal cavity of the instrument. The optical pipe is used to thermally isolate the lamp from the sensing volume. The output end of the optical light pipe is an opal glass diffuser that acts as a *quasi*-cosine (Lambertian) light source. Within the measuring volume, the first aperture on the detection side of the instrument limits the light integration to angles greater than 7°, measured from the horizontal at the opal glass. On the other side, a shadow plate limits the light to angles less than 170°. The measurement volume is defined by the intersection of this light with a viewing volume cone defined by the second and fourth aperture plates on the detection side of the instrument. The fourth aperture plate incorporates a lens to collimate the light scattered by aerosol particles so that it can be split into separate wavelengths. The nephelometer uses a reference chopper to calibrate

scattered signals. The chopper makes a full rotation 23 times per second. The chopper consists of three separate areas labelled: signal, dark, and calibrate.
The signal section simply allows all light to pass through unaltered. The dark section is a very black background that blocks all light. This section provides a measurement of the photomultiplier tube (PMT) background noise. The third section is directly illuminated this section to provide a measure of lamp stability over time. To reduce the lamp intensity to a level that will not saturate the photomultiplier tubes, the calibrate section incorporates a neutral density filter that blocks approximately 99.9 % of the incident light. To subtract the light scattered by the gas portion of the aerosol, a high-efficiency particulate air (HEPA) filter is switched in line with the inlet for 300 s every hour. This allows compensation for changes in the background scattering of the nephelometer, and in gas composition that will affect Rayleigh scattering of air molecules with time. When the HEPA filter is not in line with the inlet, a small amount of filtered air leaks through the light trap to keep the apertures and light trap free of particles. A smaller HEPA filter allows a small amount of clean air to leak into the sensor end of the chamber between the lens and second aperture. This keeps the lens clean and confines the aerosol light scatter to the measurement volume only.
Nephelometer data are corrected for angular non idealities and truncation errors according to Anderson and Ogren, 1998. Large hygroscopic effects are expected for internal RH > 60%, which can statistically occur from May to Sept. From 18.11.2009 onwards, a Nafion dryer has been installed at the inlet to measure dry aerosols. Atmospheric particle scattering coefficients presented in this report are **not** corrected for RH effects, except when specified.

Particle absorption coefficient

Aethalometer Magee AE-31 ('A' S/N 408: 0303 & 'B' S/N 740:0609)

The principle of the Aethalometer is to measure the attenuation of a beam of light transmitted through a filter, while the filter is continuously collecting an aerosol sample. Suction is provided by an internally-mounted pump. Attenuation measurements are made at successive regular intervals of a time-base period. The objectives of the Aethalometer hardware and software systems are as follows:
(a) to collect the aerosol sample with as few losses as possible on a suitable filter material;
(b) to measure the optical attenuation of the collected aerosol deposit as accurately as possible;
(c) to calculate the rate of increase of the equivalent black carbon (EBC) component of the aerosol deposit and to interpret this as an EBC concentration in the air stream;
(d) to display and record the data, and to perform necessary instrument control and diagnostic functions.

The optical attenuation of the aerosol deposit on the filter is measured by detecting the intensity of light transmitted through the spot on the filter. In the AE-31, light sources emitting at different wavelengths (370, 470, 520, 590, 660, 880 and 950 nm) are also installed in the source assembly. The light shines through the lucite aerosol inlet onto the aerosol deposit spot on the filter. The filter rests on a stainless steel mesh grid, through which the pumping suction is applied. Light penetrating the diffuse mat of filter fibers can also pass through the spaces in the support mesh. This light is then detected by a photodiode placed directly underneath the filter support mesh. As the EBC content of the aerosol spot increases, the amount of light detected by the photodiode will diminish.
For highest accuracy, we must make further measurements: the amount of light penetrating the combination of filter and support mesh is relatively small, and a correction is needed for the 'dark response signal' of the overall system. This is the electronics' output when the lamps are off: typically, it may be a fraction of a percent of the response when the lamps are on. To eliminate the effect of the dark response, we take 'zero' readings of the system response with the lamps turned off, and subtract this 'zero' level from the response when the lamps are on.

The other measurement necessary for the highest accuracy is a 'reference beam' measurement to correct for any small changes in the light intensity output of the source. This is achieved by a second photodiode placed under a different portion of the filter that is not collecting the aerosol, on the left-hand side where the fresh tape enters. This area is illuminated by the same lamps. If the light intensity output of the lamps changes slightly, the response of this detector is used to mathematically correct the 'sensing' signal. The reference signal is also corrected for dark response 'zero' as described above.
The algorithm in the computer program (see below) can account for changes in the lamp intensity output by always using the ratio quantity [Sensing]/[Reference]. As the filter deposit accumulates EBC, this ratio will diminish.
In practice, the algorithm can account for lamp intensity fluctuations to first order, but we find a residual effect when operating at the highest sensitivities. To minimize this effect and to realize the full potential of the instrument, it is desirable for the lamps' light output intensity to remain as constant as possible from one cycle to the next, even though the lamps are turned on and off again. The computer program monitors the repeatability of the reference signal, and issues a warning message if the fluctuations are considered unacceptable. When operating properly, the system can achieve a reference beam repeatability of better than 1 part in 10000 from one cycle to the next. The electronics circuit board converts the optical signals directly from small photocurrents into digital data, and passes it to the computer for calculation. A mass flow meter monitors the sampled air flow rate. These data and the result of the EBC calculation are written to disk and displayed on the front panel of the instrument.
Aethalometer data are corrected for the shadowing effect and for multiple-scattering in the filter to derive the aerosol absorption coefficient (Arnott et al., 2005) with a correction factor C = 3.65 for green light.

Multi Angle Absorption Photometer (S/N 4254515)

A new Multi Angle Absorption Photometer (MAAP) model 5012 from Thermo Scientific has been installed at the EMEP station in September 2008 and provides equivalent black carbon concentrations (EBC) and aerosol absorption (α) data at a nominal wavelength of 670 nm. Note that during a EUSSAR workshop (www.eusaar.org) in 2007 it has been observed that the operating wavelength of all MAAP instruments present at that workshop was 637 nm with a line width of 18 nm fwhm. The operating wavelength of this MAAP instrument has not been measured yet, therefore it is assumed to work at 670 nm as stated by the manufacturer.

The MAAP is based on the principle of aerosol-related light absorption and the corresponding atmospheric equivalent black carbon (EBC) mass concentration. The Model 5012 uses a multi angle absorption photometer to analyze the modification of scattering and absorption in the forward and backward hemisphere of a glass-fibre filter caused by deposited particles. The internal data inversion algorithm of the instrument is based on a radiation transfer model and takes multiple scattering processes inside the deposited aerosol and between the aerosol layer and the filter matrix explicitly into account (see Petzold et al., 2004).
The sample air is drawn into the MAAP and aerosols are deposited onto the glass fibre filter tape. The filter tape accumulates the aerosol sample until a threshold value is reached, then the tape is automatically advanced. Inside the detection chamber (Fig. 5), a 670-nanometer light emitting diode is aimed towards the deposited aerosol and filter tape matrix. The light transmitted into the forward hemisphere and reflected into the back hemisphere is measured by a total of five photo-detectors. During sample accumulation, the light intensities at the different photo-detectors change compared to a clean filter spot. The reduction of light transmission, change in reflection intensities under different angles and the air sample volume are continuously measured during the sample period. With these data and using its proprietary radiation transfer scheme, the MAAP calculates the equivalent black carbon concentration (EBC) as the instruments measurement result.

Using the specific absorption cross section σ_{BC} = 6.6 m^2/g of black carbon at the operation wavelength of 670 nm, the aerosol absorption at that wavelength can be readily calculated as:

$$\alpha = EBC \times \sigma_{BC} \qquad Eq.\ 1$$

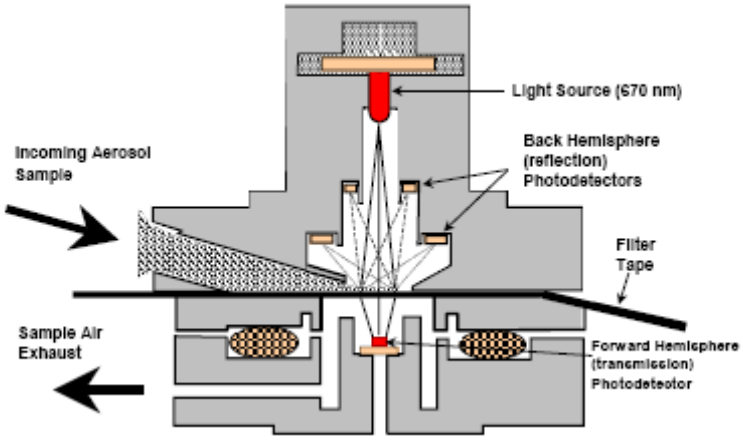

Fig. 5. MAAP detection chamber (sketch from the manual of the instrument).

Range-resolved aerosol backscattering, extinction and aerosol optical thickness

Cimel Aerosol Micro Lidar (CAML) CE 370-2 (laser & electronics: S/N 0507-846 and telescope: S/N 0507- 847)

In 2006, an aerosol backscatter LIDAR instrument (LIght Detection And Ranging) has been installed at the EMEP station for the range-resolved optical remote sensing of aerosols. It serves to bridge the gap between local, in-situ measurements of aerosols at the ground and satellite based characterizations of the aerosol column above ground. To reach this, altitude resolved aerosol backscattering, aerosol extinction and the aerosol optical thickness (AOT) are derived from LIDAR data with high time resolution.

LIDAR measurements are based on the time resolved detection of the backscattered signal of a short laser pulse that is sent into the atmosphere (for an introduction see Weitkamp, C., 2005). Using the speed of light, time is converted to the altitude where the backscattering takes place. Utilising some assumptions about the atmospheric composition, aerosol backscattering and extinction coefficients as well as aerosol optical thickness can be derived using the LIDAR equation. The received power P of the detector is therein given as a function of distance and wavelength by:

$$P(R,\lambda) = P_0 \, {}^{c\tau}\!/_{2} \, A\eta \frac{O(R)}{R^2} \beta(R,\lambda) \exp\left(-2 \int_0^R \alpha(r,\lambda) dr \right)$$

Eq. 2: P_0: Power of the laser pulse, c: speed of light, τ: laser pulse length, A: area of the telescope, η: system efficiency, R: distance, O: overlap function (between laser beam and receiving optics field of view), λ: wavelength, β: backscatter coefficient, α: absorption coefficient

LIDAR measurements were performed with a Cimel Aerosol Micro Lidar (CAML). CAML is an eye-safe, single-wavelength, monostatic aerosol backscatter lidar. The lidar emitter is a diode pumped, frequency doubled Nd:YAG laser operating at a wavelength of 532 nm, with a repetition rate of 4.7 kHz, pulse energy of 8 μJ/pulse and a width of the

laser pulse of less than 15 ns. The short integration time of the detector of 100 ns allows for a vertical resolution of 15 m. With 2048 time bins of the detector, the maximum altitude is ~30 km. However, depending on the actual atmospheric conditions and the quality of signal to noise ratio (SNR), the vertical limit for probing the atmosphere usually goes up to 15 km. Eye-safety of the system is reached by expanding the laser beam trough a 20 cm diameter, 1 m focal length refractive telescope. The emission and reception optical paths coincide through a single, 10 m long optical fibre that connects both the laser output and receiving detector with the telescope. The telescope field of view is approximately 50 μrad. The backscatter signal is sent to the receiver passing through a narrow band-pass interference filter (0.2 nm fwhm, centred at 532 nm) to reduce the background level. To avoid saturation of the detector immediately after the laser pulse is emitted and thus reduce the afterpulse signal, an acousto-optical modulator is placed before the detector that blocks the light from the detector that is directly backscattered from optical components in the light path. The detector is an avalanche photodiode photon-counting module with a high quantum efficiency approaching 55 % with maximum count rates near 20 MHz.

Data evaluation is done with an inversion algorithm based on an iteration-convergence method for the LIDAR equation (see *Eq. 2*) that has been implemented in-house using the MATLAB programming environment. Starting with the CAML raw data, the 10 minutes time averages of the backscatter profiles are space–averaged over 60 m. Then the background signal (including afterpulse component) is subtracted. The afterpulse component originates from light that is scattered back to the detector from all surfaces on the optical path to the telescope. As its intensity is rather high compared to the atmospheric backscatter, it influences the raw detector signal. Furthermore, the overlap function O(R) (see *Eq. 2*) is applied to the data before it is range corrected, i.e. multiplied by R^2. The shape of this overlap function varied significantly and thus gives rise to a potentially large error in the evaluation of the lidar data. The range corrected signal constitutes the level 0 data.
Usually, the US standard atmosphere is used to calibrate the molecular backscattering in an aerosol free region and an assumed LIDAR ratio (i.e. extinction-to-backscatter ratio) that is constant with height is used to retrieve the aerosol backscatter, extinction and optical thickness (AOT) profiles (provided as level 1 data). During 2009, the molecular extinction and backscatter profiles are computed using radiosonde measurements (launched at Linate airport) for air number of molecules. Also, instead of using a constant LR by season, the LR is determined using as a constraint the AOT measured by sun photometer.
The mean (median) estimate of the LIDAR ratios (LR) that have been used for the data inversion ranged of LR = 22.76 (17). This is a winter characteristics since the data were available over the timeframes Jan-April 2009 and Oct.-Dec. 2009.

After the Leipzig campaign (May 2009), the lidar is running for 20min and is switched off for 2 min. Thus, the cycle is 22 min. This 22 minute cycle is repeated continuously during favourable weather conditions, i.e. no precipitation and no cloud coverage that would absorb the laser pulse and thus prevent meaningful aerosol LIDAR measurements.

The number of performed measurements/total scheduled (%) for 2009 was 41/157 (26.11%). On monthly bases, the percentages of performed/scheduled measurements are as follows: 30.77, 57.14, 71.43, 7.69, 0, 0, 0, 7.14, 30.77, 53.85, 21.43, and 30.77 (Fig. 3). The retrieval of the aerosol backscatter coefficient was performed as: 30.77, 57.14, 71.43, 15.38, 0, 0, 0, 0, 30.77, 46.15, 28.57, 7.69. The statistics of the gaps in the measurements is as follows: 35% technical problems, 27% low level clouds, 23% rain and 15% other issues. The daily measurements performed within Earlinet schedule (Mondays at solar noon and solar sunset and Thursdays at solar sunset) are shown in Fig. 4.

Hygroscopicity

H-TDMA

The H-TDMA instrument was made of DMA1, selecting particles of a given dry (<20% RH) diameter, a pre-humidifier in the aerosol flow, which can be by-passed, DMA2, in which the sheath air is humidified to get a RH inside DMA2 as close as possible to 90% RH (Figure 6). Humidification the sheath air in DMA2 is obtained by circulating water at 10 - 25°C in the counter-flow channel of a Nafion dryer. RH is measured in DMA2 sheath air (using an RH probe). The measurement of RH in DMA2 sheath air is used to control the water bath temperature in order to keep RH constant at 90%.

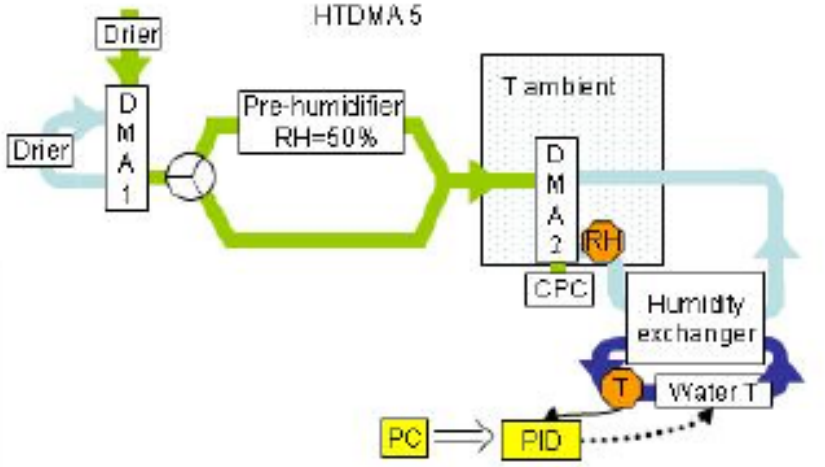

Fig. 6. Sketch of the H-TDMA set-up used for aerosol hygroscopic growth measurements in 2008 – 2009.

Thus, the days with measurements performed are 5-31 May 2008 (87,1%), 1-20 June 2008 (66.67%), 4-25 July 2008 (70.97%), 16-30 September 2008 (50%), 1-17 October 2008 (54.84%), 2-12 December 2008 (35.48%), 22-31 January 2009 (32.26%) and 1-2 February 2009 (7.14%). The days covered by measurements are shown in Fig 4.

Sampling and off-line analyses

Particulate Matter

PM2.5 from quartz fibre filters

PM2.5 was continuously sampled at 16.7 L/min on quartz fibre filters with a Partisol sampler equipped with carbon honeycomb denuder and a PM10 + cyclone with cut @ 2.5 µm sampling head. The sampled area is 42 mm Ø in both samplers. Filters were from PALL Life Sciences (type TISSUEQUARTZ 2500QAT-UP). Filter changes occurred daily at 08:00 UTC.
Filters were weighed at 20 % RH before and after exposure with a microbalance Sartorius MC5 placed in a controlled (dried or moisture added and scrubbed) atmosphere glove box. They were stored at 4 °C until analysis.
Main ions (Cl^-, NO_3^-, SO_4^{2-}, $C_2O_4^{2-}$, Na^+, NH_4^+, K^+, Mg^{2+}, Ca^{2+}) were analysed by ion chromatography (Dionex DX 120 with electrochemical eluent suppression) after extraction of the soluble species in an aliquot of 16 mm Ø in 20 ml 18.2 MOhm cm resistivity water (Millipore mQ).

Organic and elemental carbon (OC+EC) were analysed using a Sunset Dual-optical Lab Thermal-Optical Carbon Aerosol Analyser (S/N 173-5). PM2.5 samples were analysed using the EUSAAR-2 thermal protocol that has been developed to minimize biases inherent to thermo-optical analysis of OC and EC (Cavalli et al., 2009):

Fraction Name Sunset Lab.	Plateau Temperature (°C)	Duration (s)	Carrier Gas
OC 1	200	120	He 100%
OC 2	300	150	He 100%
OC 3	450	180	He 100%
OC 4	650	180	He 100%
cool down		30	He 100%
EC1	500	120	He:O_2 98:2
EC2	550	120	He:O_2 98:2
EC3	700	70	He:O_2 98:2
EC4	850	80	He:O_2 98:2

PM10 from quartz fibre filters

PM10 was usually sampled 4 times per month for a 24 h period at 16.7 L/min on quartz fibre filters (TISSUEQUARTZ 2500QAT-UP) with a Partisol Plus 2025sampler using a PM10 sampling head. Filter preparation and analysis has been performed exactly as described above for PM2.5 samples to check for differences in the chemical composition of coarse particles compare to PM2.5.In total, 35 filters have been sampled and analyzed.

Wet-only deposition

For the precipitation collection, two Eigenbrodt wet-only samplers (S/N 3311 and 3312) were used that automatically collect the rainfall in a 1 L polyethylene container. The collection surface is 550 cm^2. 24-hr integrated precipitation samples (if any) are collected every day starting at 8:00 UTC. All collected precipitation samples were stored at 4 °C until analyses (ca. every 3 months).
Analyses include the determinations of pH and conductivity at 25 °C with a Sartorius Professional Meter PP-50 and principal ion concentrations (Cl^-, NO_3^-, SO_4^{2-}, $C_2O_4^{2-}$, Na^+, NH_4^+, K^+, Mg^{2+}, Ca^{2+}) by ion chromatography (Dionex DX 120 with electrochemical eluent suppression).

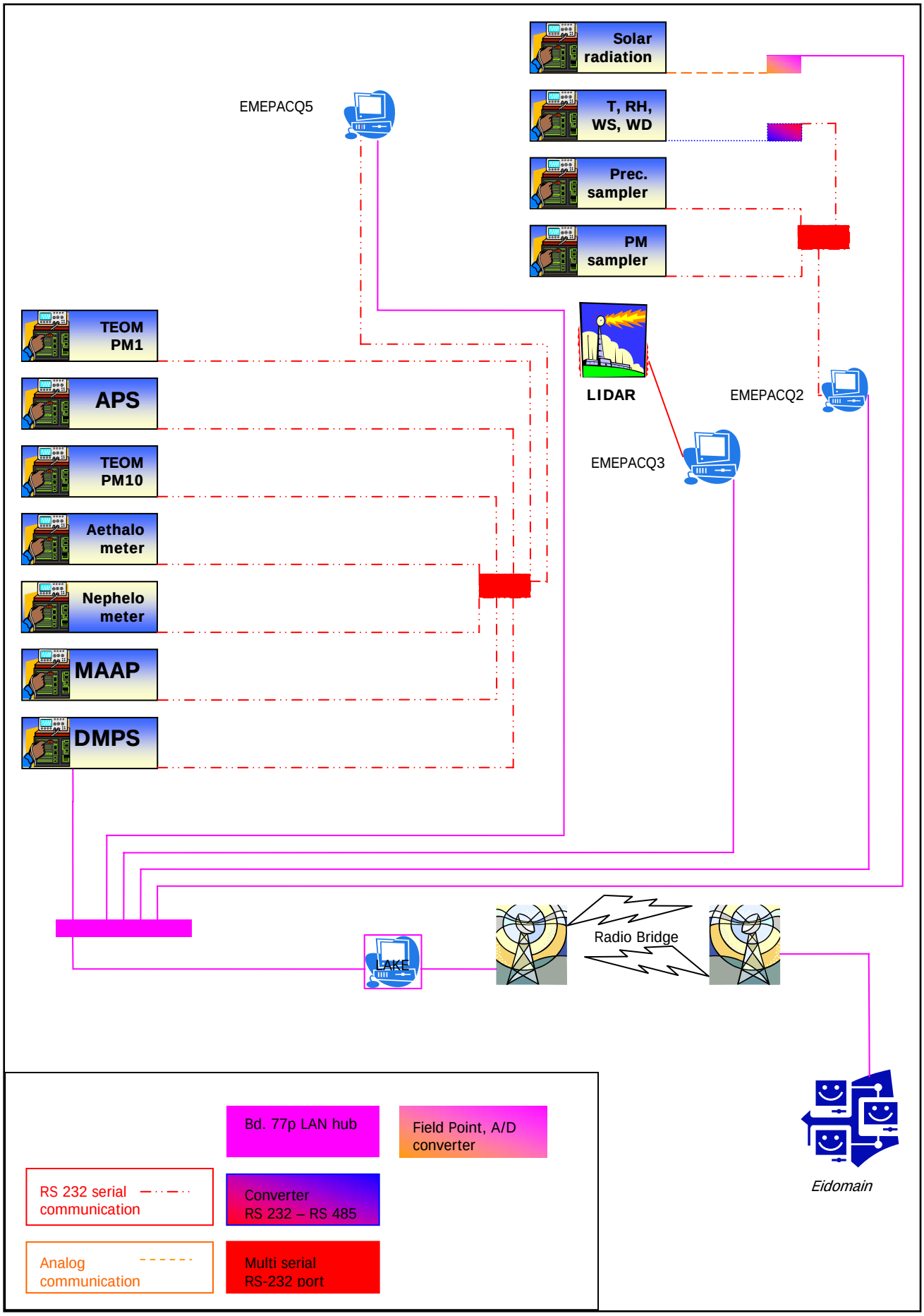

Fig. 7. Set-up of the EMEP GAW station Data Acquisition System

On-line data acquisition system

Main differences between the 2008 and 2009 versions of the ”on-line data acquisition system”: In respect to 2008, gas phase data were not acquired, so no web page was displayed. Regarding the data acquisition, signal converters CAS24 RS232-485 for TEOM and National Instrument e-net 485 for Aethalometer were removed, since it was tested and demonstrated the RS-232 signal is strong enough to pass from one container to the other.

The JRC EMEP-GAW station Data Acquisition System (DAS) is a specifically tailored set of hardware and software (implemented by NOS s.r.l), designed to operate instruments, acquire both analog and digital output from instruments and store pre-processed measurement data into a database for further off-line evaluation. The DAS operated and controlled the instrumentation during 2009, software bug fixed and updates were implemented when necessary.

The software environment of the DAS is Labview 7.1 from National Instruments and the database engine for data storage is Microsoft SQL Server 2005.

The DAS is designed to continuously run the following tasks:

- Start of the data acquisition at a defined time (must be full hour);
- Choose the instruments that have to be handled;
- Define the database path where data will be stored;
- Define the period (10 minutes currently used) for storing averaged data, this is the data acquisition cycle time;
- Obtain data (every 10 seconds currently set) for selected instruments within the data acquisition cycle:
  - For analog instruments (currently only the CM11 and CMP11 Pyranometers), apply the calibration constants to translate the readings (voltages or currents) into analytical values;
  - Send commands to query instruments for data or keep listening the ports for instruments that have self defined output timing;
  - Scan instruments outputs to pick out the necessary data;
- Calculate average values and standard deviations for the cycle period;
- Query instruments for diagnostic data (when available), once every 10 minutes;
- Store all data in a database
  - With a single timestamp for the gas analyzers, FDMS-TEOM and Nephelometer
  - With the timestamp of their respective measurement for all other instruments.

The following instruments are managed with the DAS, using two PCs (currently called emepacq2 and emepacq5):

Emepacq5:

- Number size distribution for particles diameter >0.500 µm, APS
- On-line PM10 mass, FDMS-TEOM
- On-line PM1 mass, FDMS-TEOM
- Aerosol light absorption, Aethalometer
- Aerosol light absorption, MAAP
- Aerosol light scattering, Nephelometer

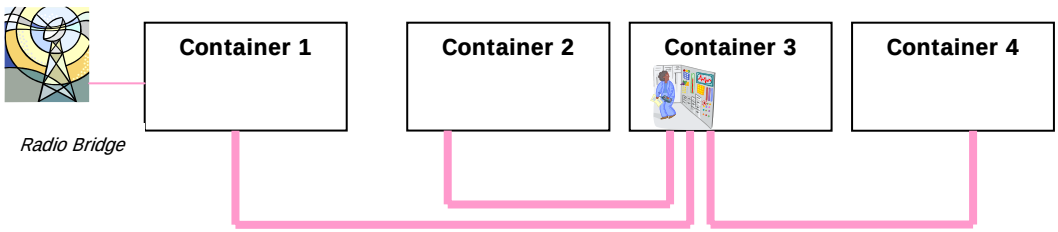

.

Fig. 8. Interconnections of the laboratory container at the EMEP station

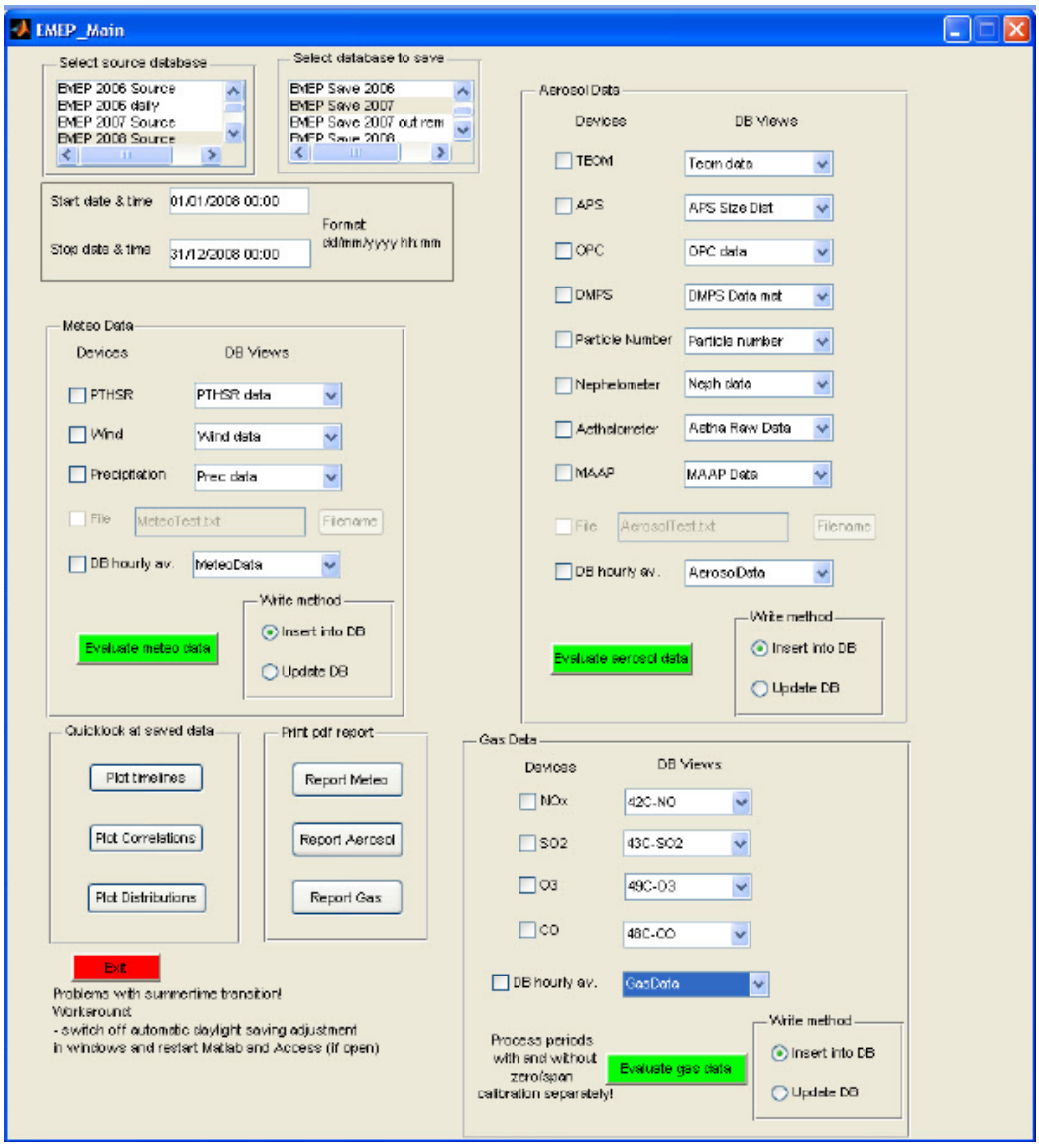

Fig. 9. Graphic user interface of the EMEP data evaluation program.

Emepacq2:

- Solar radiation
- Weather transmitter (temperature, pressure, relative humidity, wind speed and direction, precipitation)
- Precipitation data
- Particulate matter sampling data

A third PC (**emepacq3**) is dedicated to operate the LIDAR system, a fourth PC (**emepdma**) to operate the DMPS and to store its data directly to the database.

Data acquired with "emepacq5" are currently stored on the central database **EmepDB** hosted on the PC **Lake**. Data acquired with "emepacq2" are locally stored on the same PC in a database called **EmepDB** as well. The PC "**Lake**" also connects the laboratory to the JRC network (Eidomain) via a radio bridge. The schematic setup of the data acquisition system is shown in Fig. 7.
The four containers at building 77p that make up the EMEP station are connected to each others by user configurable point-to-point lines (see Fig. 8).
Trough these point-to-point connections, data are exchanged via TCP-IP and RS232 protocols, depending on the instruments connected to the lines.
The acquisition time is locally synchronized for all PCs via a network time server running on lake and is kept at UTC, without adjustment for summer/winter time. Data are collected in a Microsoft SQL Server 2005 database, called EmepDB.db that runs on "**Lake**". This database is nightly backed-up by the IES back-up service.

Data evaluation

For evaluating the 2009 data, the structured data evaluation system (EMEP_Main.m) with a graphic user interface (see Fig. 9) has been used with Matlab Release R2007b (www.mathworks.com) as the programming environment. The underlying strategy of the program is:

1) Load the necessary measurement data from all selected instruments from the data acquisition database as stored by the DAS (source database).
2) Apply the necessary individual correction factors, data analysis procedures, etc. specific to each instrument at the time base of the instrument.
3) Perform the calculation of hourly averages for all parameters.
4) Calculate results that require data from more than one instrument.
5) Store hourly averages of all results into a single Microsoft Access database, organized into different tables for gas phase, aerosol phase and meteorological data (save database).

Only the evaluation of gas phase data has an automatic removal algorithm for outliers / spikes implemented: d_i = 10 minute average value at time i, std_i = standard deviation for the 10 minute average (both saved in the raw data)

if $std_i > 100 \cdot \overline{std}$ and $|d_i - d_{i\pm1}| > 10 \cdot \overline{std}$

$\rightarrow d_i = 1/2\left(d_{i-1} + d_{i+1}\right)$ for d_{i-1} **and** d_{i+1} **no** outliers, otherwise $d_i = missig\ data$.

This algorithm corrects for single point outliers and removes double point outliers. All other situations are considered correct data. To check these data and to exclude outliers for all other measurements, a manual inspection of the hourly data needs to be performed.

In addition, quick looks of evaluated data for selected time periods can be produced as well as printed timelines in the pdf-format for the evaluated data. All database connections are implemented via ODBC calls to the corresponding MS Access database files.
With a second program (EMEP_DailyAverages.m), daily averages (8:00 < t ≤ 8:00 +1 day) of all parameters stored in the hourly averages database can be calculated and are subsequently stored in a separate MS Access database.

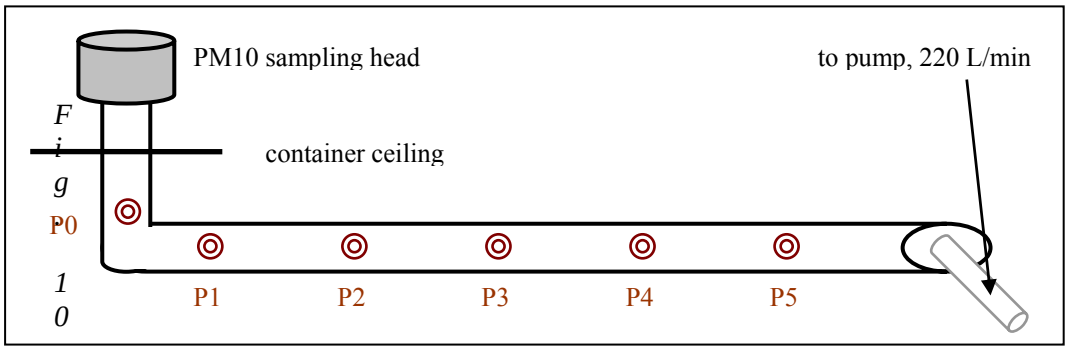

Fig. 10. Sketch of the new aerosol inlet in container IV indicating the sampling points Px (see Table 2 for information about the sampling points).

New container and sampling conditions

Since 2008, all instruments but one FDMS-TEOM (*S/N 140AB233870012*) for the physical characterization of aerosols operated in the new laboratory container IV at the EMEP station that is located north-west of the existing containers: Aethalometer, Nephelometer, Aerodynamic Particle Sizer, Differential Mobility Particle Sizer, Multi-Angle Absorption Photometer, Tapered Element Oscillating Mass balance and LIDAR.
A new inlet tube system (Aluminium): diameter: 15 cm, length of horizontal part: ~280 cm, vertical part: ~220 cm) has been constructed that allows each instrument to draw its required sample isokinetically from the main inlet tube. A sketch of the inlet is shown in Fig. 10. The flow rate to the external pump is 230 L/min to ensure a laminar flow. Sampling point positions for the different instruments are indicated in the sketch as well and described in Table 2. The FDMS-TEOM and MAAP instruments that are also located in container IV use their own inlet systems.

Table 2. Sampling points of the inlet system.

sampling point	approx. distance to sampling head [cm]	instruments connected	flow to instrument [L/min]
P0	200	APS	5.0
P1	270	CPC	1.0
P2	320	DMPS	1.0
P3	375	Aethalometer A	2.5
P4	425	Aethalometer B	2.5
P5	480	Nephelometer	20 / 5.3

The size dependent particle losses along the tube radius are shown in Gruening et al., 2009). Measurements using ambient aerosols have been performed simultaneously with the two DMPS again at the sampling points P0 and P2 for different radial positions relative to the tube centre (0, 40 and 52 mm) at P2. A small loss of particles towards the rim of the tube can be observed, but it stays below 15 %. The bigger deviation for particles smaller than 20 nm is again a result of very small particle number concentrations in this diameter range and thus rather big counting errors.

During December 2009 a sampling condition monitoring system has been installed at the aerosol inlet. Since then temperature and relative humidity for the main inlet, DMPS inlet, Aethalometer inlet and Nephelometer inlet are measured and saved into the EMEP database.

Quality assurance

At JRC level the quality system is based on the Total Quality Management philosophy, the implementation of which started at the Environment Institute in December 1999. Lacking personnel to specifically follow this business, the JRC-Ispra station for atmospheric research did not renew the accreditation for the monitoring of SO_2, NO, NO_2 and O_3 under EN 45001 obtained in 1999. However, most measurements and standardized operating procedures are based on recommendations of the EMEP manual (1995, revised 1996; 2001; 2002), WMO/GAW 153, ISO and CEN standards. Moreover, the JRC-Ispra gas monitors and standards are checked by the European Reference Laboratory for Air Pollution (ERLAP) regularly (see specific measurement description for details). For on-line aerosol instrumentation in 2009, two intercomparisons took place at the world calibration center for aerosol physics (WCCAP) in Leipzig (D) in the frame of EUSAAR (www.eusaar.org): one for DMPS in June 2009 in Leipzig where new DMPS system constructed according to EUSAAR specifications were tested, and a second one at the beginning of July 2009, during which absorption/scattering of particles issues were addressed. At the second intercomparison, also the two Aethalometers participated.

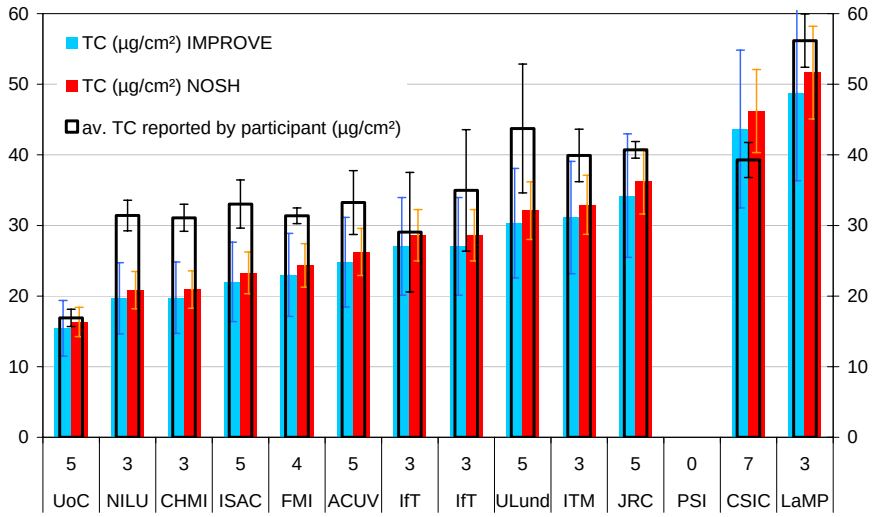

Fig. 11. *TC amounts determined by the EUSAAR partners and reference values. Also shown are the uncertainties of these values (the blue IMPROVE and red NOSH are the NIST values).*

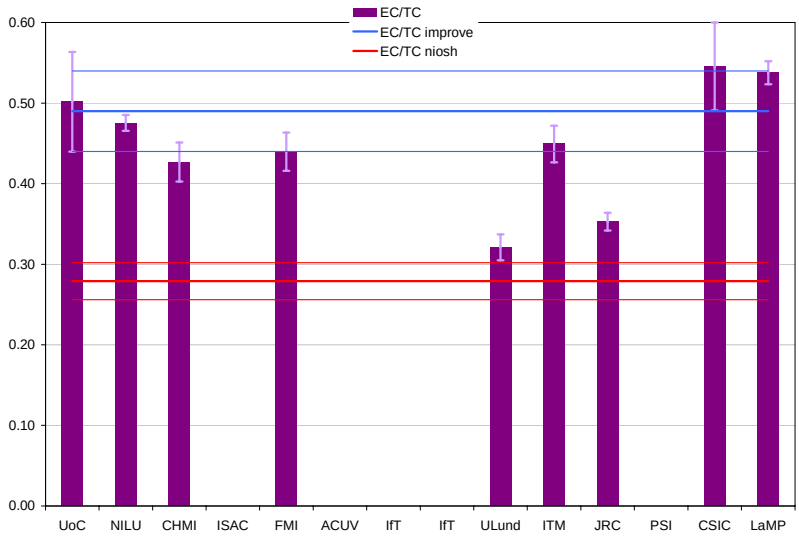

Fig. 12. EC/TC ratios and standard deviations reported by EUSAAR partners, together with NIST information values for this ratio, determined with two protocols commonly used in the USA.

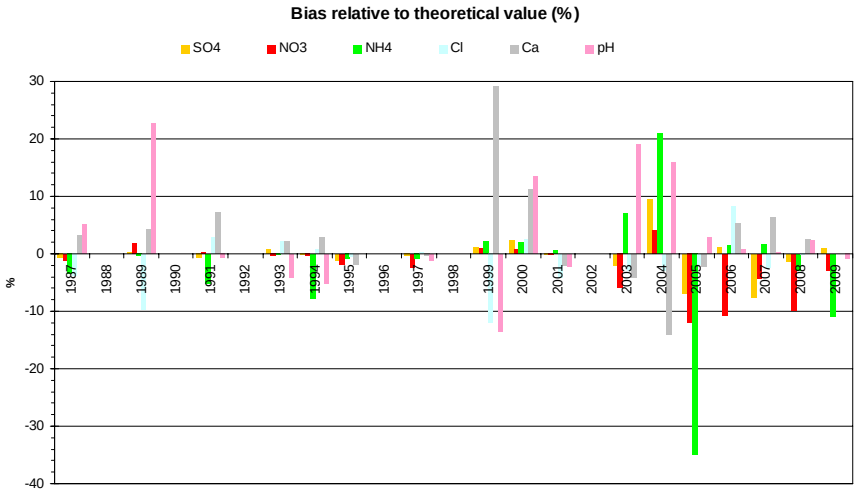

Fig. 13. JRC-Ispra results of the EMEP intercomparison for rainwater analyses (1987-2009).

In addition, most of the other instruments were regularly calibrated through maintenance contracts. For the analysis of total, organic and elemental carbon (TC, OC and EC, respectively), a Round Robin test including EUSAAR partners has been organized by the JRC-Ispra. In 2009 the intercomparison was based on NIST (USA – National Institute of Standards and Technology) reference materials 8785, for which reference values for TC amounts were available. This round robin test did not allow us to gain any information relative to the accuracy of TC determination by each Eusaar partner. As shown in Figure 11 most participants found TC amounts larger than the NIST reference values (shown by blue and red) raising doubts on the validity of the reference TC values assigned to the materials. The exercise also showed that partner using the EUSAAR_2 protocol obtained EC/TC ratio for the same reference material differing by a factor of 1.7. This is an unsuccessful result.

The results of the JRC-Ispra station's participation in the yearly EMEP intercomparison exercise for rainwater analyses are shown in Fig. 13. Due to the use of new IC calibration standards since 2006, the bias for the different analytes in the last years' EMEP laboratory intercomparisons have been reduced drastically compared to the years before.

Data quality for other measurements is also checked whenever possible through comparison among different instruments (for gases), mass closure (for PM) and ion balance (for precipitation) exercises.

Station representativeness

The representativeness of the JRC-EMEP station has been evaluated to check:

- what area are the data currently acquired at the EMEP station representative for?
- would a move from the actual location to building 51 (or to "Roccolo hill, nido blu" 150 m from building 51 on Rocolo hill) lead to a break in the data series collected during the past 2 decades?

To address these questions, three sets of parallel measurement campaigns were performed in February-March 2006, February-March 2007 and July 2008 at the EMEP site (building 77p) and at building 51. The two sites are ~1.4 km apart, bld. 77p along "via perferica nord" and bld. 51 on the top of the "Roccolo" hill, outside the JRC fence. Also the altitude of the two sites differs: 209 m a.s.l. for bld. 77p, 269 m a.s.l. for bld. 51. Bd. 77p is located close to a pond and a swampy area of the JRC forest in a remote area with very limited car passages. High trees are present which does not agree with the EMEP recommendations for the choice of a good of sampling site. The laboratory in building 51 is located at the third floor of the building itself, where more than 20 people work. It is close to the treetop canopy in the north sector, while the south sector has an open view. Sampling at bd. 77p was performed at 3 m above the ground, while at bld.51 sampling was done with a 1.5 m inlet above the rooftop. During the first two campaigns, only ozone has been monitored. In 2008 SO_2 was also added. Data has been evaluated taking also different meteorological situations (with different T, RH, WS, WD) into account. Observations are discussed in details in *Dell'Acqua et al.*, 2010.

Summarizing, no relevant difference in the daily maximum concentration of the compared parameters has been observed. However, daily minimum are generally lower at the current site compared to Bd. 51 on Rocolo hill. Therefore a move of the EMEP measurement site from the current location to building 51 (or to "Roccolo hill, nido blu" close to bulding 51) would enlarge the spatial representativeness of the station, but probably not imply any large discontinuity in the data series. The fact that O_3 daytime maximum concentrations are very similar at the EMEP-GAW station compared to the top of another JRC building (Bd. 51) located 50 m higher in the Roccolo locality also indicates that there are no significant local sources of O_3 precursors at the site. However, O_3 minima and SO_2 concentrations in general are lower at the EMEP-GAW station during both winter and summer periods, suggesting stronger sinks at the EMEP site.

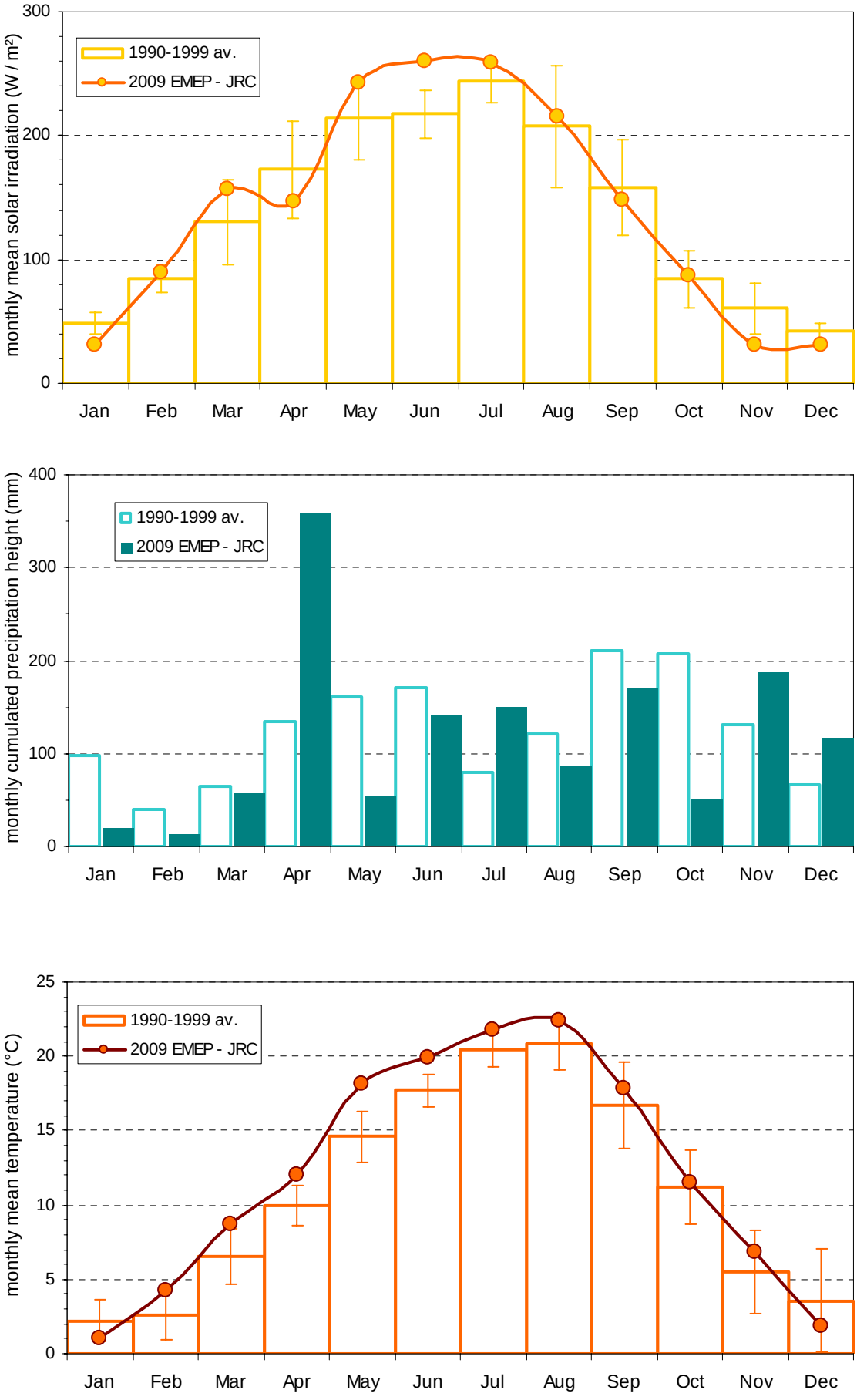

Fig. 14. Solar global irradiation, precipitation amount, and temperature monthly means observed at the EMEP station in the JRC-Ispra in 2009, compared to the 1990-1999 period ± standard deviations.

Results of the year 2009

Meteorology

Meteorological data were acquired directly at the EMEP site using the Vaisala WXT510 weather transmitter. 14 shows monthly values of meteorological parameters for 2009 compared to the 1990-1999 average used as reference period.

The monthly averaged solar radiation for 2009 follows the 1990-1999 average, with May - July significantly sunnier and November cloudier than during the reference period “1990-1999 average”.

The total rainfall accumulated to 1408 mm, i.e. only 5 % less compared to the 1990-1999 average (1484 mm). Only January and February were very dry, April had comparably much more precipitation compared to the “1990-1999 average”.

2009 was a rather warm year, with only the months of December and January slightly cooler than during the reference period “1990-1999 average”. The temperature average over the whole year of 2009 was 12.2 °C compare to 11.0 °C during 1990-1999.

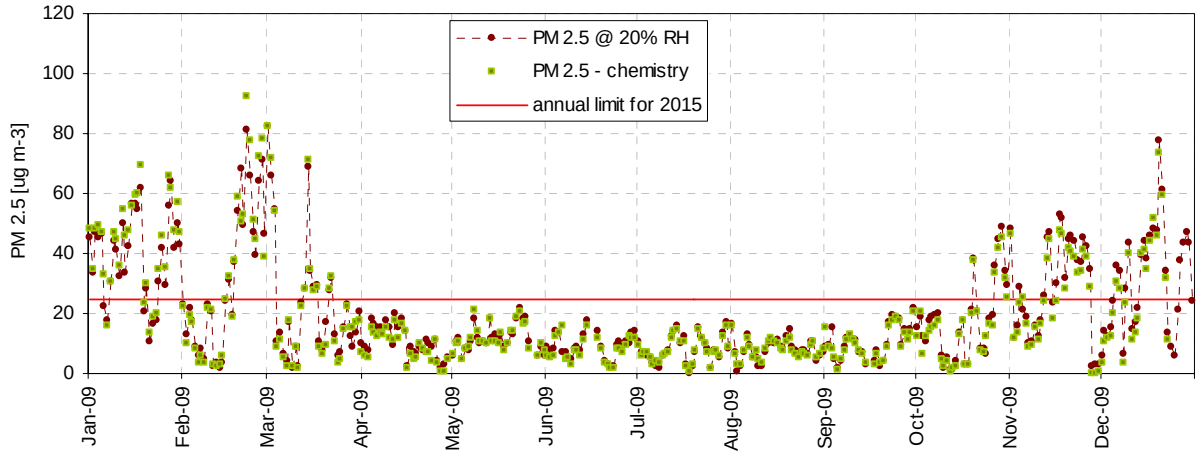

Fig. 15. 24hr-integrated PM2.5 mass concentrations from off-line gravimetric measurements at 20% RH in 2009.

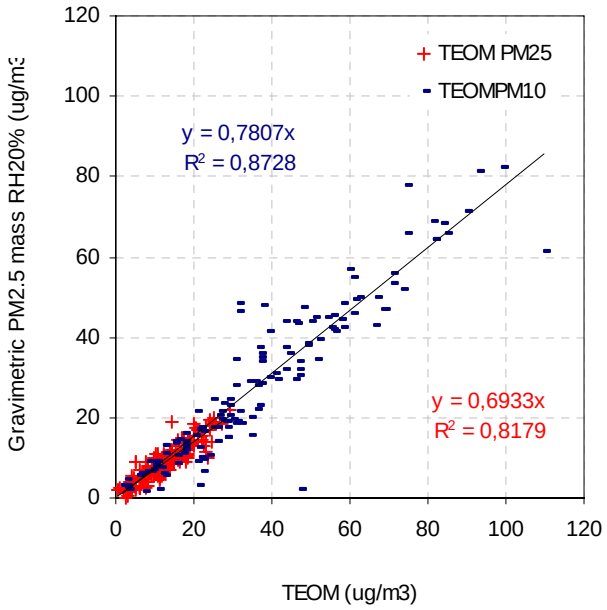

Fig. 16. Regressions line between FDMS-TEOM PM10 and gravimetric PM2.5 measurements at 20 % RH.

Particulate phase

Particulate matter mass concentrations

The two FDMS-TEOMs were measuring PM10 from 01.01.2009 to 31.03.2009. The regression with hourly values between the two is represented by the regression TEOM_B=0.86*TEOM_A+4.64, R^2=0.88. Afterwards TEOM_A (s/n 233870012) was measuring PM2.5 from 01.04.2009 to 31.12.2009, and TEOM_B (s/n 253620409) was measuring PM1 from 01.04.2009 to 31.12.2009. PM2.5 annual mean concentrations (Fig. 15) were 19.0 µg/m³ measured gravimetrically at 20 % RH and 19.9 µg/m³ from FDMS-TEOM. The gravimetric value was similar to the one measured in 2008 of 19.3 µg/m³. It can be observed that the last two years, the PM2.5 values were well below the European annual limit value of 25 µg/m³ that has to be reached by 2015 (European directive 2008/50/EC).

The artefact taken into account by the FDMS-TEOM PM2.5 for the period April to December ranged from -11.8 (July) to +1.6 (September) over 24 hr and averaged -3.6 µg/m³. On an hourly basis, sampling artefacts ranged from -55 to +37 µg/m³, spikes excluded.

Comparing the PM10 mass measured with the FDMS-TEOM to gravimetric PM2.5 mass at 20 % RH (Fig. 16) suggests that PM2.5 contributes with about 80 % to the total PM10 mass. The correlation with R^2 = 0.78 is comparable to the last years. The comparison of the PM2.5 mass measured with the FDMS-TEOM to gravimetric PM2.5 mass at 20 % RH (see also Fig. 16) shows that the gravimetric PM2.5 only can account for about 70 % of PM2.5 measured by FDMS-TEOM. It seems like FDMS-TEOM PM2.5 overestimates the mass, because the ratio extinction to mass for FDMS-TEOM PM2.5 is 3.9. This value is rather low, potentially indicating that this mass is too high (see p. 45-46). The same ratio for FDMS-TEOM PM10 is 4.3, more reasonable. In the current report, the gravimetric PM2.5 mass concentration is used for further assessments.

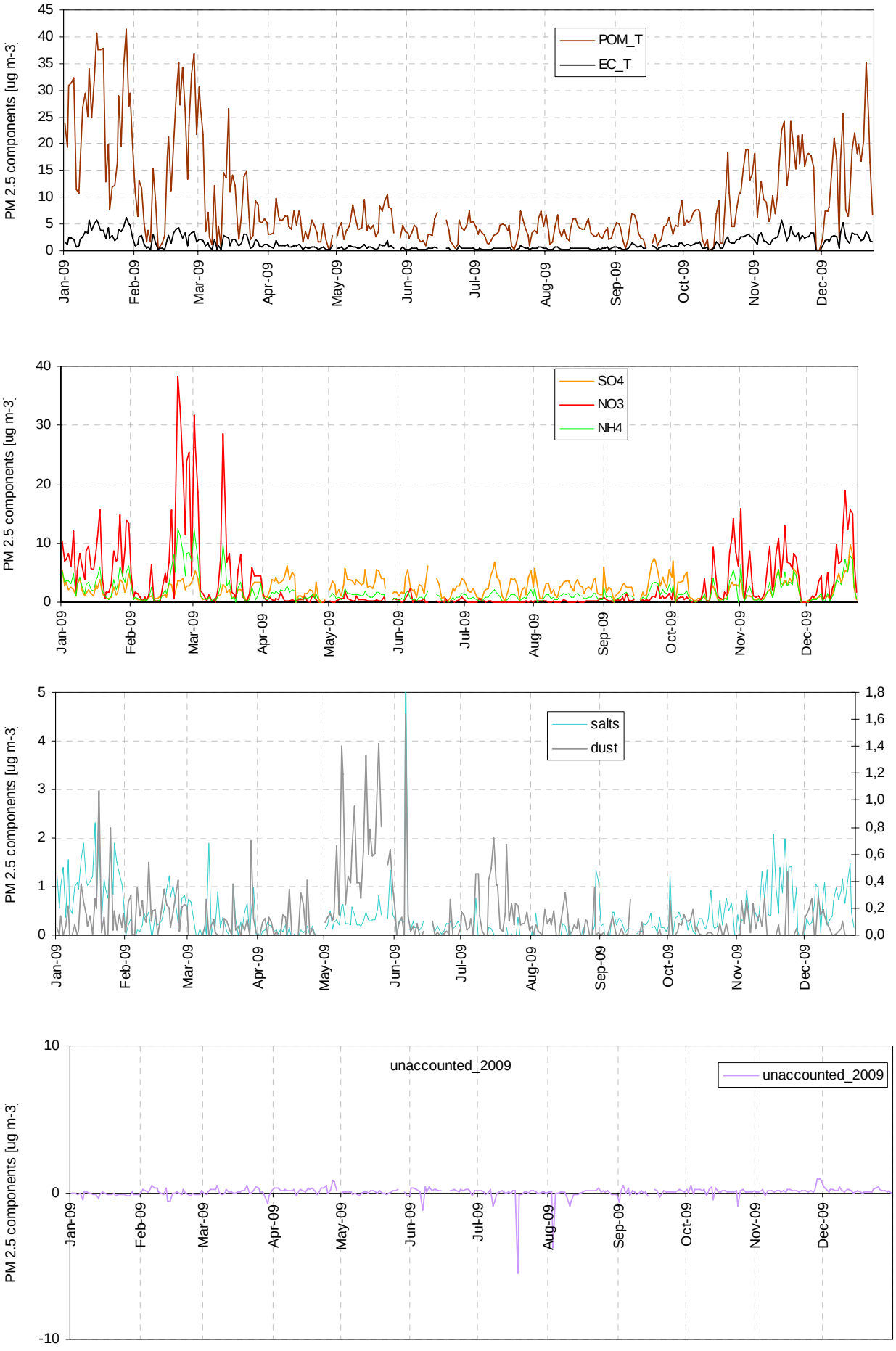

Fig. 17. 24-hr integrated concentrations of the main aerosol components in PM2.5 during 2009.

PM2.5 chemistry:

Main ions (Cl^-, NO_3^-, SO_4^{2-}, $C_2O_4^{2-}$, Na^+, NH_4^+, K^+, Mg^{2+}, and Ca^{2+}), OC and EC were determined from the quartz fibre filters (for the whole year) collected for PM mass concentration measurements.

Fig. 17 shows the temporal variations in the PM2.5 main components derived from these measurements. Particulate organic matter (POM) is calculated by multiplying OC (organic carbon) values by the 1.4 conversion factor to account for non-C atoms contained in POM (Russell et al., 2003). "Salts" include Na^+, K^+, Mg^{2+}, and Ca^{2+}. Dust is calculated from Ca^{2+} concentrations and the slope of the regression found between ash and Ca^{2+} in the analyses of ash-less cellulose filters (Whatman 40) in previous years (4.5). Most components show seasonal variations with higher concentrations in winter and fall, and lower concentrations in summer, like PM2.5 mass concentrations. This is mainly due to changes in pollutant horizontal and vertical dispersion, related to seasonal variations in meteorology (e.g. lower inversion layer in the winter season). The amplitude of the POM, NH_4^+ and NO_3^- seasonal cycles may be enhanced due to equilibrium shifts towards the gas phase, and/or to enhanced losses (negative artefact) from quartz fibre filters during warmer month.

NH_4^+ follows NO_3^- + SO_4^{2-} very well as indicated by the regression shown in Fig. 18. This correlation results from the atmospheric reaction between NH_3 and the secondary pollutants H_2SO_4 and HNO_3 produced from SO_2 and NO_x, respectively. The slope of this regression is very close to 1, which means that NH_3 was sufficiently available in the atmosphere to neutralise both H_2SO_4 and HNO_3. This furthermore indicates that PM2.5 aerosol was generally not acidic in 2009.

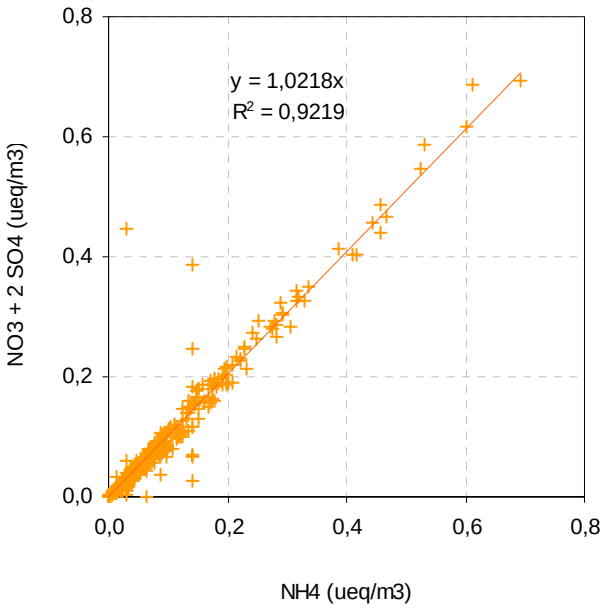

Fig. 18. SO_4^{2-} + NO_3^- vs. NH_4^+ (µeq/m³) in PM2.5 for 2009.

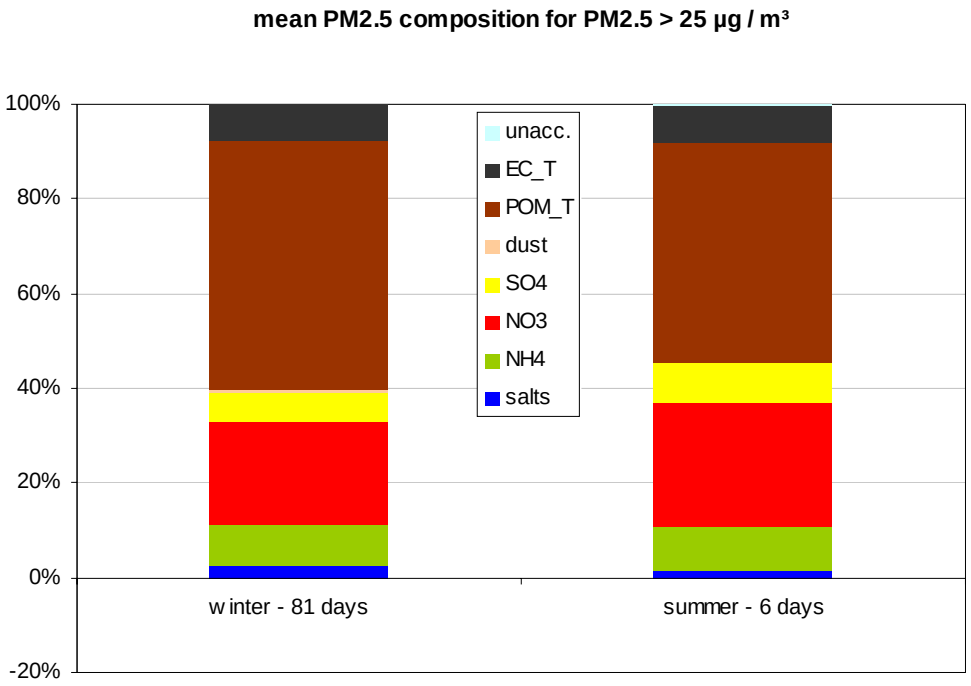

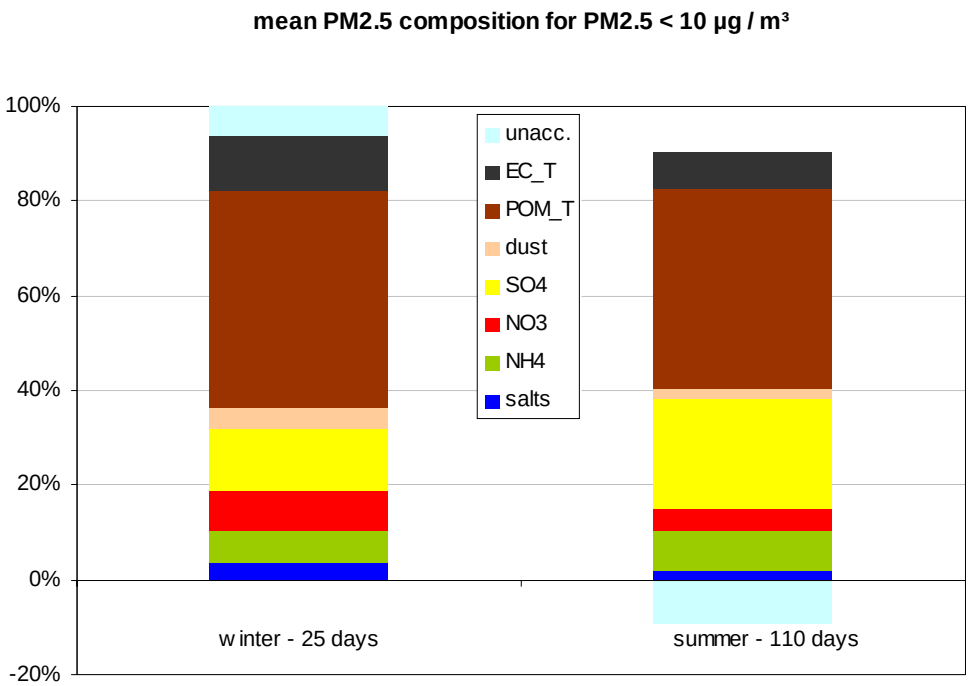

Fig. 19. Average composition of PM2.5 for days during which PM2.5 > 25 µg/m³(top) and PM2.5 < 10 µg/m³(bottom), in winter (Jan., Feb., Dec.) and extended summer (Apr. – Oct.)

Contribution of the main aerosol components in PM2.5

The contributions of the main aerosol components to PM2.5 are presented in Fig. 19 (a) for days on which the "24-hr limit value for PM2.5 of 25 µg/m³ was exceeded" in winter (Jan., Feb., March, Nov. and Dec., 81 cases) and extended summer (Apr. to Oct, 6 cases) and (b) for days on which 24-hr integrated PM2.5 concentration was below 10 µg / m³ in winter and in extended summer.

These PM2.5 compositions may not always represent accurately the actual composition of particulate matter in the atmosphere (due to various sampling artefacts), but are suitable to assess which components contributed to the PM2.5 mass concentration when collected according to the normative rules described in EN14907.

Over the whole year 2009, carbonaceous species accounted for 55% of $PM_{2.5}$ (EC: 8%, POM: 47%), and secondary inorganics for 37% (NH_4: 9%, NO_3: 10%, and SO_4:18%). Mineral dust and sea-salt like species accounted for 2% each. In both winter and (extended) summer, particulate air pollution days are characterised by a strong increase in NO_3 contribution, and to a lesser extent of POM contribution. Considering low PM 2.5 concentration days, summertime is characterised by higher SO_4^{2-} concentrations (faster SO_2 photochemical conversion) and lower NO_3^- concentrations ($HNO_3 + NH_3 \leftrightarrow NH_4NO_3$ equilibrium moves towards the gas phase as temperature increases).

Dust and salts do not contribute significantly to the PM2.5 mass as these aerosols are not predominant in the Po valley region and are also more likely found in the coarse particle fraction.

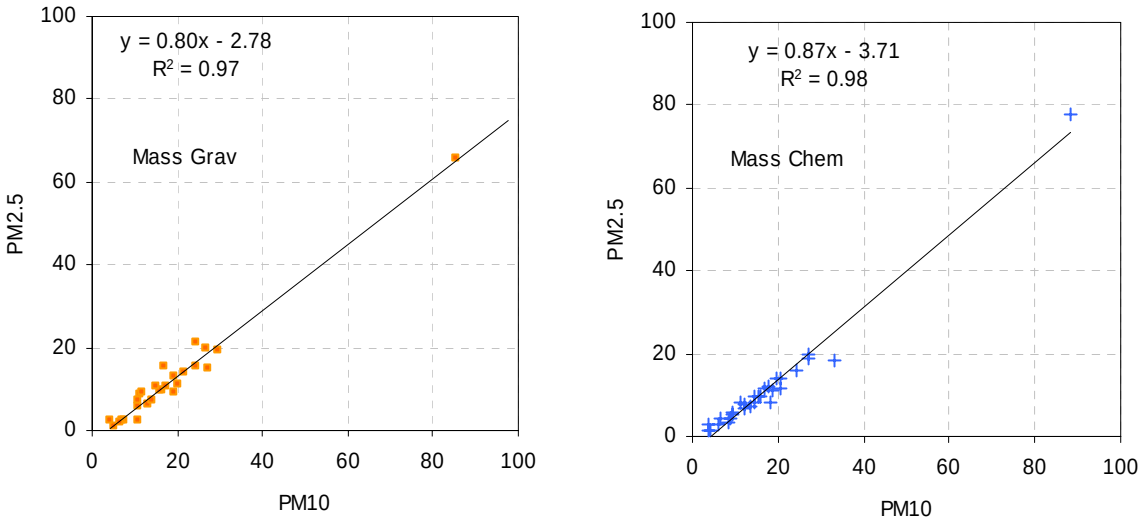

Fig. 20. Regression line between weighted PM10 and PM2.5 at 20% RH and regression line between chemical masses of PM10 and PM2.5.

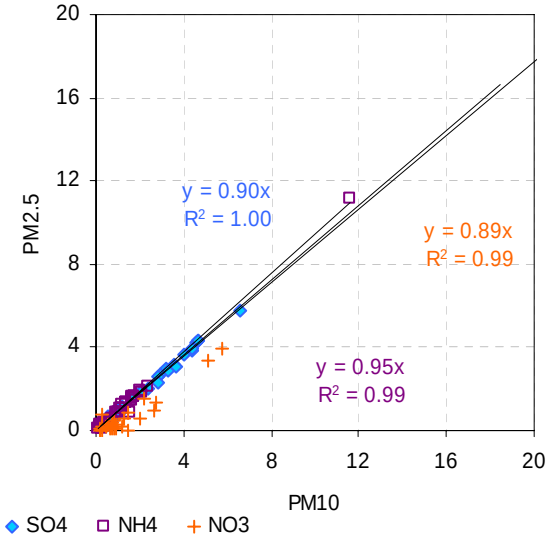

Fig. 21: Correlation between chemical components (NH_4, SO_4 and NO_3) of PM10 and PM2.5.

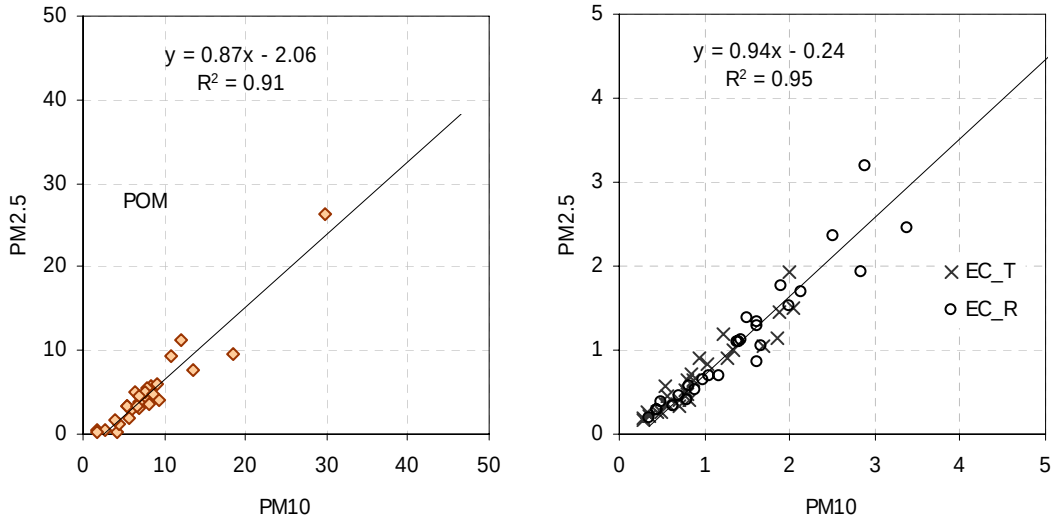

Fig. 22 : Correlation between chemical components (POM and EC) of PM10 and PM2.5

PM10 chemistry

PM10 has been collected and analyzed for a total of 35 filters in 2009. Comparing weighted masses of PM2.5 and PM10, it shows that PM2.5 makes up for about 82 % of the total PM10 mass (Fig. 20). For the chemical masses, PM2.5 accounts for about 90 % PM10 (Fig. 20).

Furthermore, looking at the chemical analysis of the PM10 and PM2.5 filters, the correlations of Fig. 21 indicates that the contribution of (NH_4, SO_4 and NO_3) to PM10 and PM2.5 are rather similar (about 90 – 95 % are found in PM2.5).

In addition, when comparing PM2.5 to PM10 filters, Fig. 22 indicates that the contribution of POM from PM2.5 to PM10 is ca. 87% and that the one of EC is 94%.

These observations show a good consistency between PM_{10} and $PM_{2.5}$, which indicate that no critical problem in filter sampling occurred over 2009. They also suggest that losses of semi-volatile inorganics (namely NH_4NO_3) are NOT significantly increased by the use of the OC denuder.

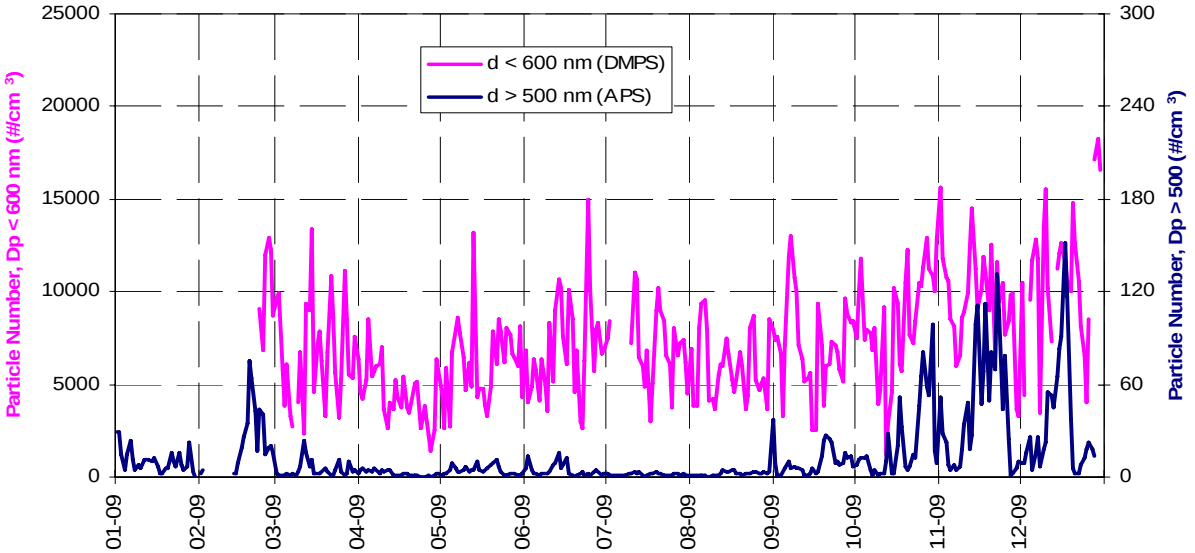

Fig. 23. 24 hr - averaged particle number concentrations for Dp > 500 nm and Dp< 600 nm

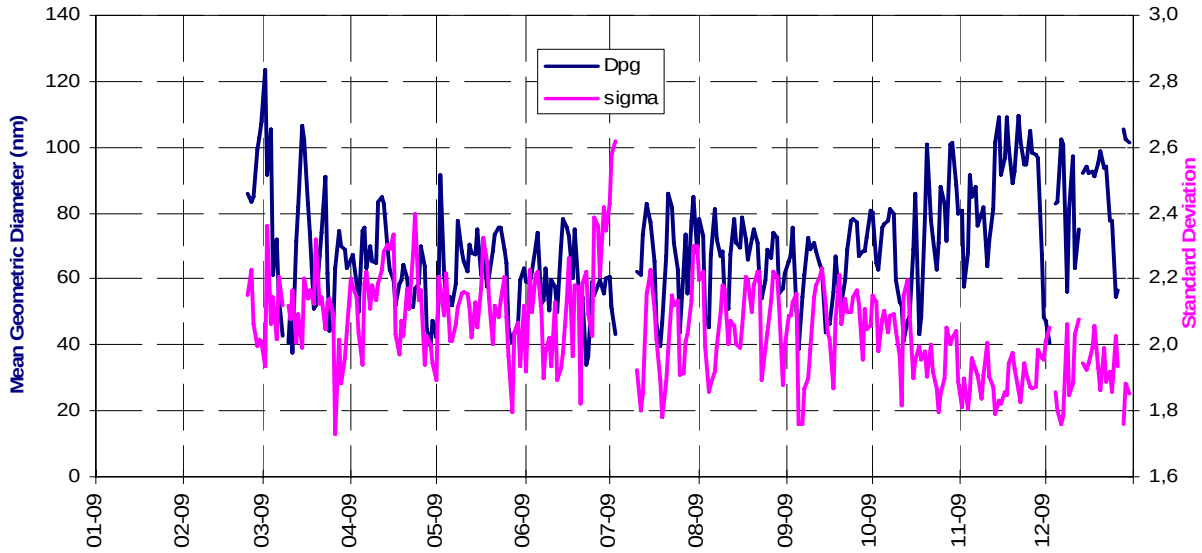

Fig. 24. 24 hr - averaged particle geometric mean diameter (measured with DMPS) and standard deviation

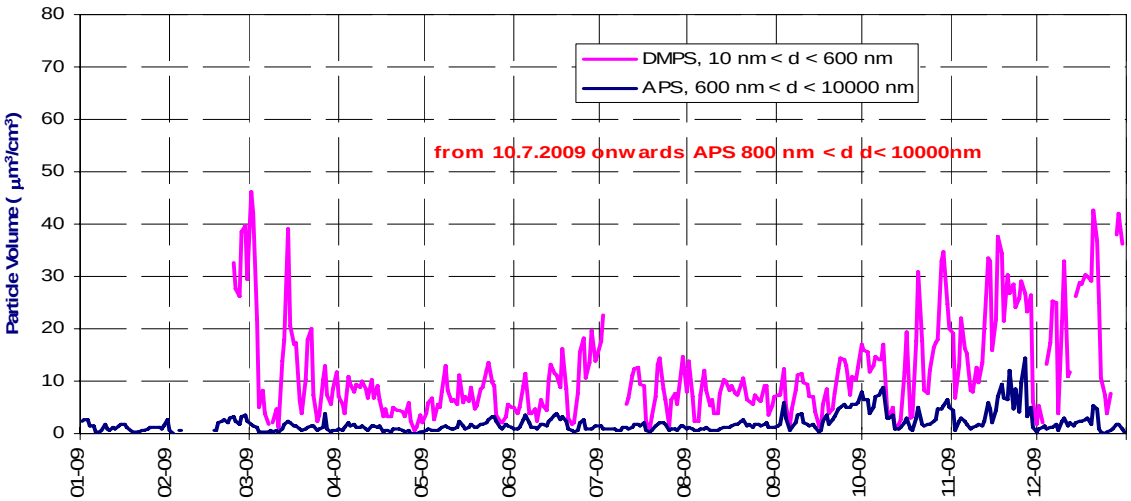

Fig. 25. 24 hr - averaged particle volume concentrations for Dp > 600 nm and Dp < 600 nm until 12.6.2009 and for Dp > 800 nm and Dp < 800 nm thereafter.

Aerosol physical properties

Measurements of the particle number size distributions smaller than 600 nm (until 12.06.2009 or smaller than 800 nm (after 12.06.2009) diameter were carried out using a Differential Mobility Particle Sizer from 23.02.2009 and the rest of the year 2009. Particle number concentrations averaged over 24 hr (from 08:00 to 08:00 UTC) ranged from 1200 to 18300 cm^{-3} (average: 7400 cm^{-3}) and followed a seasonal cycle comparable to that of PM mass concentration, with maxima in winter and minima in summer (Fig. 23).

The variations in particle size distributions parameters at RH < 30 % (Fig. 24) show seasonal patterns as well: the mean geometric diameter is generally larger in winter than in summer, whereas the standard deviation of the distribution follows an opposite trend (larger in summer than in winter). The size distribution of particles larger than 500 nm was measured using an Aerodynamic Particle Sizer (aerodynamic converted to geometric diameter using a particle density of 1.50). As previously observed, particles larger that 500 nm accounted for a very small fraction of the total particle number only, on average for 0.1 % (Fig. 23), but for about 8 % of the total particle volume (Fig. 25). The seasonal variations in particle volume concentration reflect the changes in particle number and mean geometric diameter, with larger volumes in winter than in summer.

Looking at particle number size distributions reveals clear inconsistencies (could be 1 order of magnitude in counting around 600 nm) between the APS and the DMPS across the 2 first thirds of the year (see Fig. 26, p. 40), but the problem disappeared in Autumn(from 29 Oct.) when APS A (S/N 70535014) was calibrated by TSI.

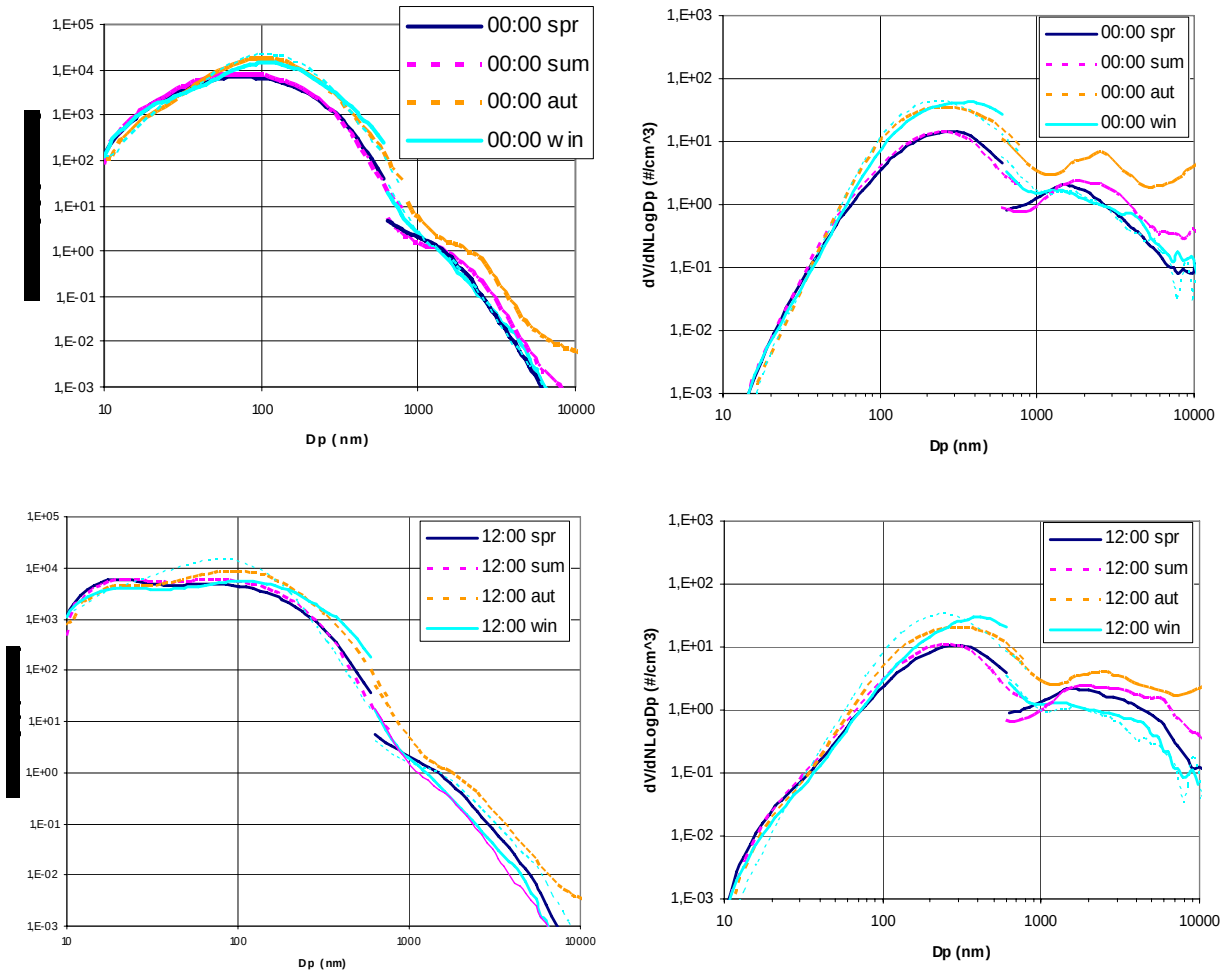

Fig. 26. Seasonal mean particle number (left) and volume (right) size distributions at 00:00 (top) and 12:00 UTC (bottom) measured with a DMPS (10-600 nm solid lines, 10-800 nm dashed lines) and an APS (0.6-10 µm solid lines, 0.8-10 µm dashed lines, density of 1.5 g/cm3 assumed for conversion of aerodynamic diameter)

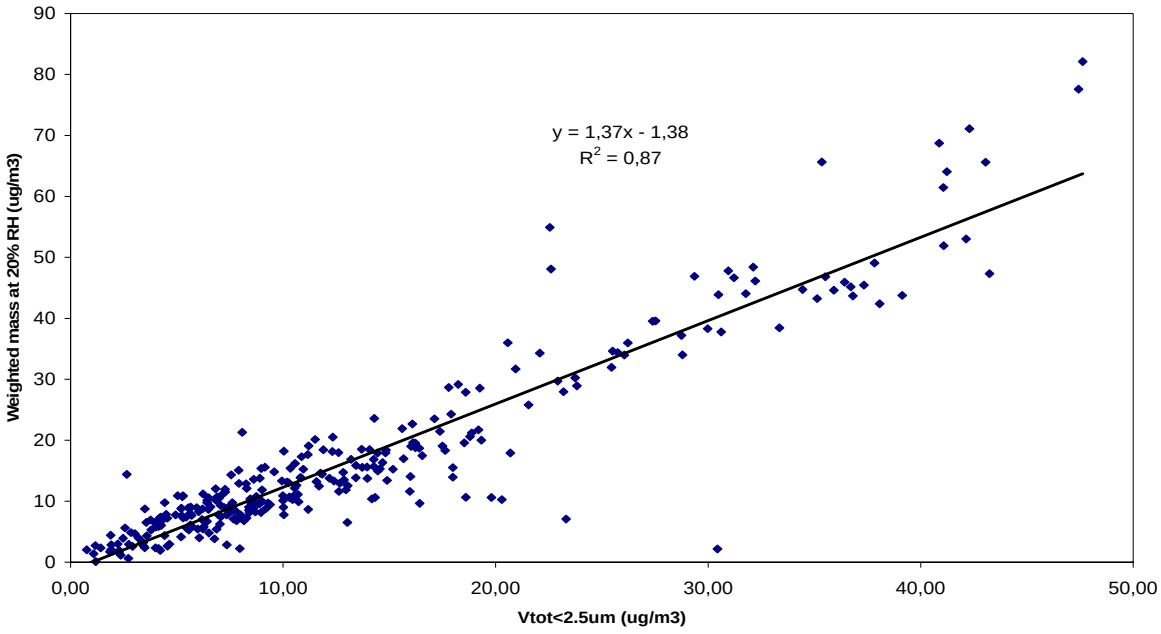

Fig. 27. Regressions line between PM2.5 mass concentrations determined from gravimetric measurements at 20 % RH and particle volume (Dp < 2.5 µm) calculated from DMPS and APS measurements

The comparison between PM2.5 mass and aerosol volume concentration (for Dp < 2.5 μm) shows a good correlation (Fig. 27). The slope of the regression between PM2.5 at 20 % RH and particle volume suggests an aerosol density close to 1.37, slightly higher than 1.25 measured in 2008. It should be mentioned that a density factor in the range of 1.6 ± 0.1 is normally considered for atmospheric aerosols (McMurry et al., 2002).

Particles bigger than 600 nm make up for only about 16 % of the total volume, compared to 24 % in 2008.

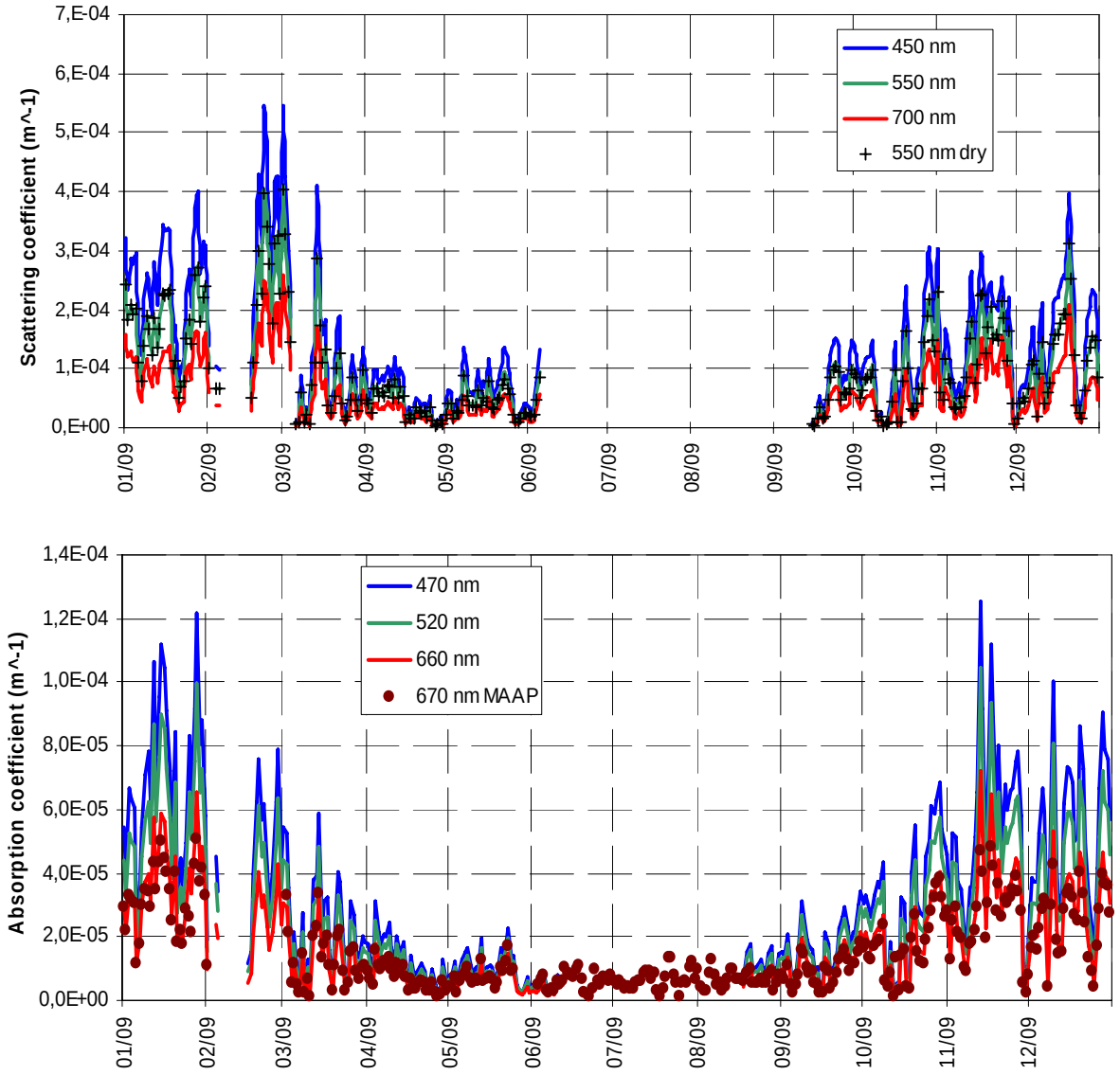

Fig. 28. Daily mean atmospheric particle scattering (top) and absorption (bottom) coefficients at three wavelengths, derived from Nephelometer and Aethalometer/MAAP measurements (not corrected for RH, except if specified)

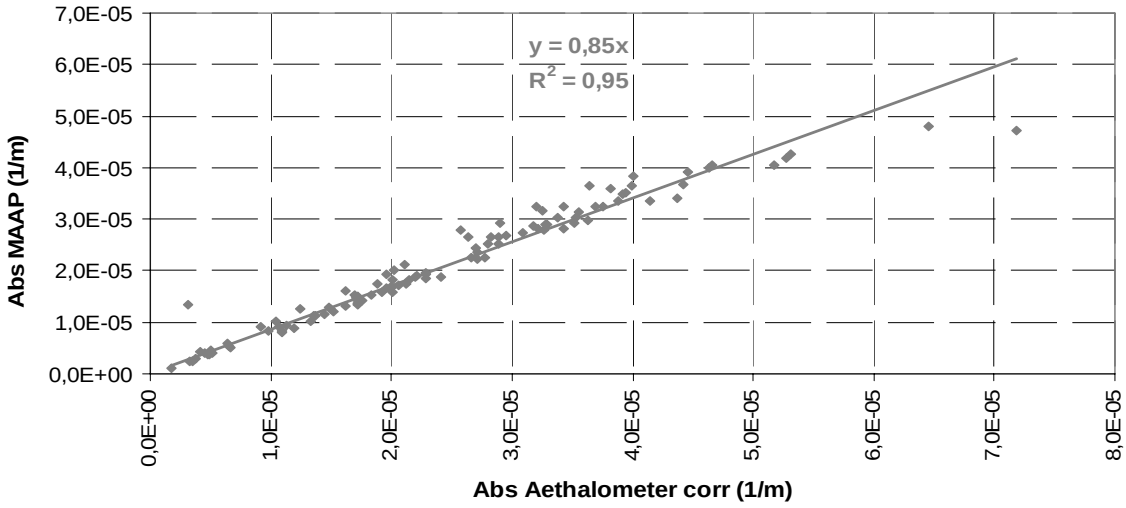

Fig. 29. Comparison of Aethalometer and MAAP derived absorption at 660 and 670 nm, respectively. Data are hourly averages and straight line is fitted to absorption <= 4E-5 (1/m).

Aerosol optical properties

Aerosol optical properties have been monitored continuously during 2009 (Fig. 28). Measurements with the Nephelometer were not performed during an extended instrumental service period (June till mid-September). Data from the Nephelometer TSI 3563 have been corrected for angular non idealities (truncation to 7 – 170°, slightly not cosine-weighted distribution of illumination) according to Anderson and Ogren (1998). The equations linking the correction factor and the Ångstrom coefficient established for sub-µm particles (Anderson and Ogren, 1998) were used for correcting total scattering, since the median sub-µm mass fraction was 0.88 in Ispra for 2009. This leads to quite conservative corrections (on average +7 %, min: +3 %, max: +13 % for scattering, ca -5 % for backscattering) However, the Nephelometer was operated without RH control until 18.11.2009, when a Nafion dryer has been installed at the inlet. But the RH inside the Nephelometer was recorded during the entire year. It was observed that the RH in the Nephelometer exceeded 60 % only for a total of just 9 hourly averages in May. At such a RH, scattering coefficients are 25 % larger than in dry conditions, based on calculations accounting for a mean refractive index derived from chemical composition, the Ångstrom coefficient, and the Mie theory (Nessler et al., 2005). For 2009, corrections for RH were <11 % for 99 % of all hourly and 24-hr averaged values.

Atmospheric particle absorption coefficients were derived from the Aethalometer AE-31 data corrected for the shadowing effect when Nephelometer data were available, and for the multiple scattering occurring on/into the Aethalometer filter according to Schmid et al. (2006). Corrections for the shadowing effect were +5 % on average (< +11 % for 90^{th} percentile). Therefore, possible biases in scattering coefficient determination are not expected to affect the determination of the aerosol absorption coefficient significantly.

The uncertainty of the multiple scattering correction factor may introduce a much larger uncertainty in the aerosol absorption coefficient values, since correction factors ranging from 2 to 4 have been proposed (Weingartner et al., 2003; Arnott et al., 2005). The correction factors we used were 3.6, 3.65 and 3.95 for blue, green and red light, respectively.

It should be noted that the use of the correction coefficients proposed by Schmid et al. (2006) leads to aerosol absorption coefficients equal to 82 % of the PSAP-matched aerosol absorption coefficients calculated from the regression found in the Aethalometer manual (version 2003.04, p.11): PSAP abs. coef. [Mm^{-1}] = 10.78 EBC [$\mu g\ m^{-3}$].

The absorption coefficient has been calculated from the equivalent black carbon concentration (EBC) using the specific absorption cross section of 6.6 m^2/g as stated in the manual of the MAAP instrument.

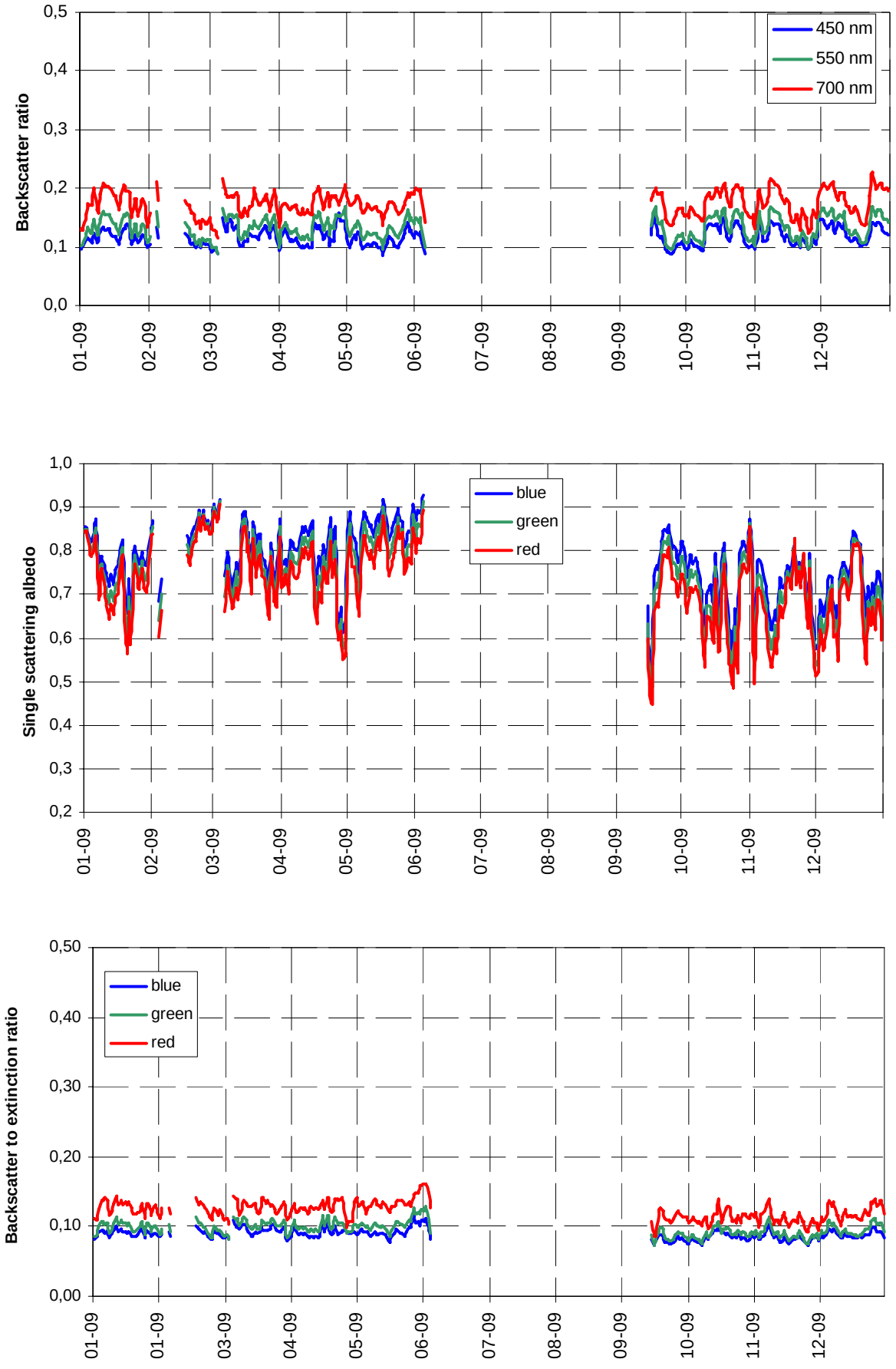

Fig. 30. Aerosol 24-hr average backscatter to total scatter ratio, single scattering albedo and backscatter to extinction ratio at three wavelengths corresponding to blue, green and red (RH generally < 40%).

Both scattering and absorption coefficients follow seasonal variations (Fig. 28) in line with PM mass variations, mainly controlled by pollutant dispersion rates.

In Fig. 29 the hourly averages of the aerosol absorption coefficient measured with the Aethalometer (λ = 660 nm, corrected as described above) and with the MAAP (λ = 670 nm) are shown. The first order polynomial fit has been done to all data. It shows an excellent agreement between the Aethalometer and MAAP instruments (slope = 0.85, R^2 = 0.95) for small absorption values, i.e. low equivalent black carbon concentrations of up to ~6 $\mu g/m^3$. For larger values though, the MAAP deviates from the Aethalometer, and significantly underestimates the absorption. This behaviour strictly depends on the aerosol absorption and not on instrumental parameters such as the filter loading.

The backscatter / total scatter ratio generally ranged from ca. 10 to ca. 30 % (Fig. 30). The 24 hr averaged single scattering albedo at λ = 550 nm (at RH generally <40 %) ranged from 0.49 to 0.91 (annual average 0.75), with generally higher values in summer compared to winter. The aerosol extinction coefficient was calculated as the sum of the scattering and absorption coefficients. Compared to the 2008 measurements, no significant change in optical particle properties has been observed during 2009.

The aerosol extinction coefficient and particle mass or volume concentrations are rather well correlated (Fig. 31). The slope of the regression between extinction and mass shows that the extinction mass efficiency is on average 4.5 m^2g^{-1}, giving an excellent agreement with 4.4 m^2 g^{-1}, the value calculated based on the aerosol mean chemical composition during 2009, and mass cross section coefficients for the various constituents found in the literature (Table 3). The slope of 6.9 of the extinction to volume correlation, together with the extinction to mass ratio (6.9/4.7 = 1.47), agrees rather well with the aerosol particle density of 1.37 found in Fig. 27).

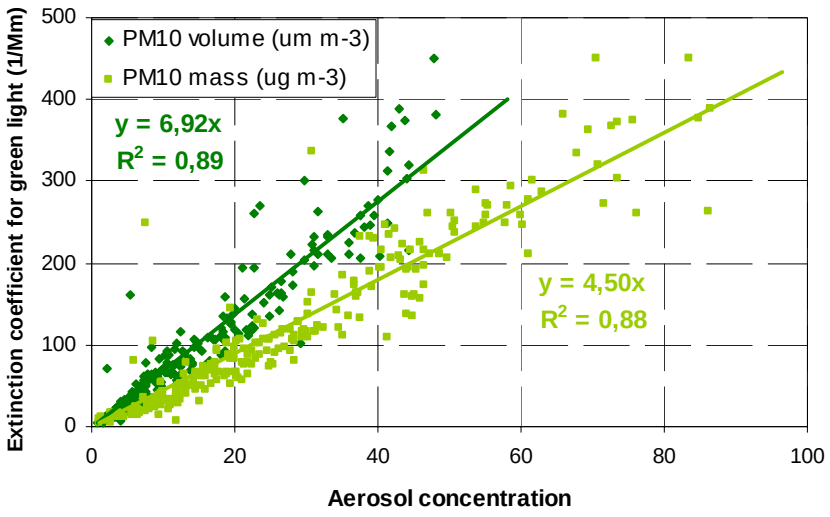

Fig. 31. Regression lines between the aerosol extinction coefficient and PM10 mass (FDMS-TEOM) and volume (DMPS + APS) concentrations. PM10 mass data from Jan., Feb. and March 2009.

	2009 PM2.5 comp. (%)	σ_{ext} (m^2/g)	Reference (for σ_{ext})
"sea salt"	2	1.3	Hess et al., 1998
NH_4^+, NO_3^- and SO_4^{2-}	37	5.0	Kiehl et al., 2000
organic matter	47	3.6	Cooke et al., 1999
black carbon	8	11	Cooke et al., 1999
Dust	2	0.6	Hess et al., 1998
Total	**100**	**4.4**	

Table 3. Mean aerosol chemical composition (PM2.5) in 2009 and extinction efficiency.

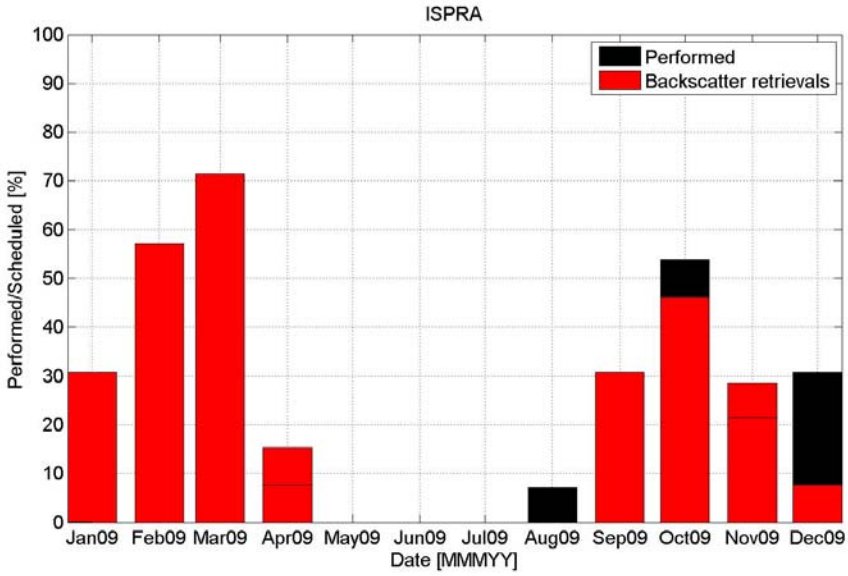

Fig. 32. Performed/scheduled measurements for 2009 (black) and backscatter coefficient retrievals/scheduled measurements (red).

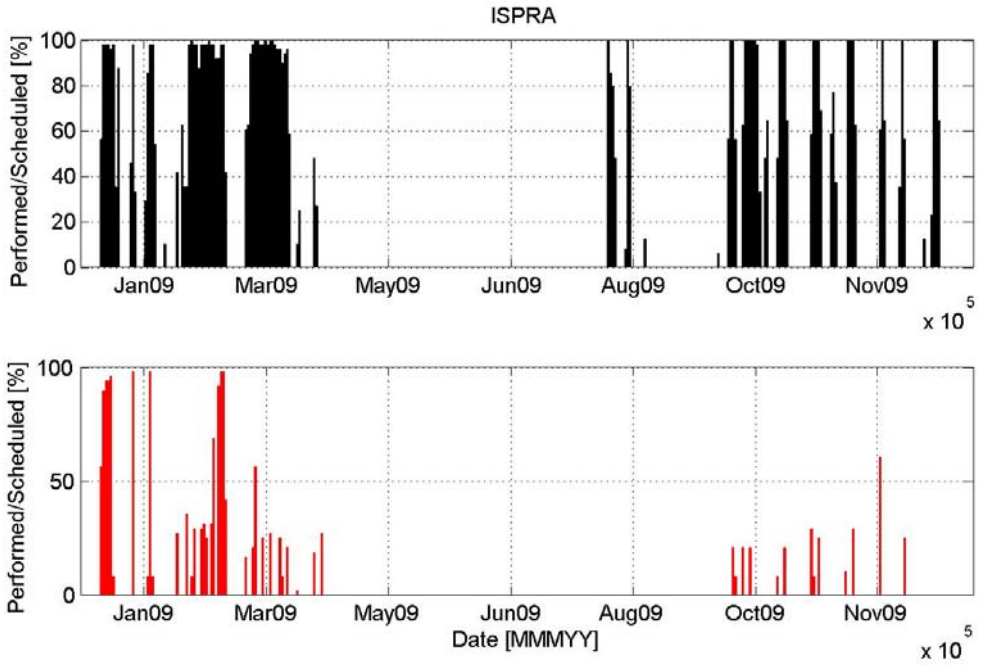

Fig. 33. Performed/scheduled measurements for 2009 (upper plot) and backscatter coefficient retrievals/scheduled measurements (lower plot), on daily basis

.

LIDAR measurements – *v*ertical profiles of aerosol optical properties

Aerosol backscatter and extinction profiles have been derived from CIMEL LIDAR measurements in 2009, whenever the weather situation was favourable, i.e. no rainfall and no low clouds present. During May 2009, the lidar was deployed in Leipzig, Germany, for participation within the EARLI09 campaign (EArlinet Reference Lidar Intercomparison 2009). Thus, from mid-April to mid-June, the lidar was not available for routine measurements for Earlinet schedule and Calipso overpasses.

After lidar return from Leipzig (May 2009), a series of tests and change of various parts took place. Thus, a considerable part of the gaps in the scheduled measurements is due to technical/instrumental problems. From 157 scheduled measurements (following the Ealinet schedule), there were 41 performed measurements (26.1%) and 38 retrieved backscatter coefficients (24.2%). The percentages per months are shown in Fig. 32. The data upload to Earlinet database is completed for 2009.

The Cimel lidar was intended to run continuously. The daily measurements were performed in proportion of 23.2% with respect to the Earlinet schedule. Statistics on daily basis are shown in Fig. 33. Note that the percentage of the backscatter coefficient retrieval is usually smaller than the percentage of the performed to the scheduled measurements and this is due to the fact that not all the measured profiles are suitable for the inversion (in order to obtain the backscatter coefficient).

Below, we make a brief presentation of the Leipzig campaign and of the CAML performance. One of the main objectives of EARLINET-ASOS is to assure the quality of the lidar measurements of all EARLINET-ASOS stations by means of direct lidar system inter-comparisons with approved reference lidar systems, and by means of controlled regular internal quality checks. The EARLI09 campaign in Leipzig was the first step of the direct lidar system inter-comparisons. During this campaign the EARLINET-ASOS reference lidar systems have been approved and the internal quality-check tools have been tested. The reference lidar systems are expected to measure at the three "standard" backscatter and two Raman wavelengths and must be mobile. In a second step each EARLINET-ASOS station will be compared to one of the mobile reference lidars in 2009 and 2010 (http://www.earli09.earlinet.eu/). CAML system participated along with other ten lidar system from Europe. The campaign, weather permitting, consisted in two intensive measurements sessions (usually 3 hours each) per day: one during day time and one during night time. The comparisons are made for individual signals, as average over a certain time interval (e.g. 30 min., 60 min.) and for the coarser resolution within the systems, which was 60 min. Raw data are acquired at 1 min. interval. The measurements over the entire campaign were performed over 12 days, with a total number of 21 sessions.

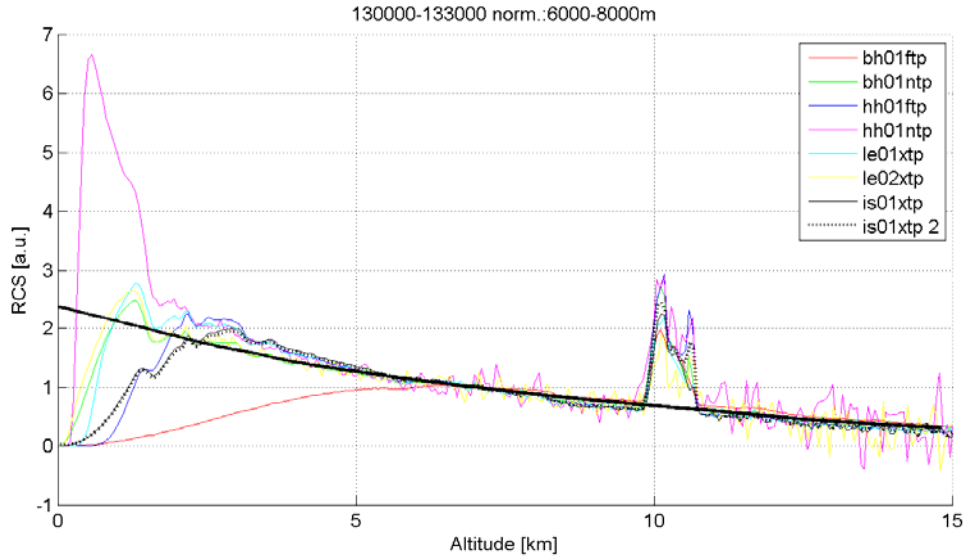

Fig. 34. Normalized RCS, day time measurements on 12 May. The title shows the interval for averaging (13:00:00-13:30:00 UTC) and the normalization region (6000-8000m). The thick black curve represents the normalized RCS corresponding to the molecular profile. The two is01 lines represent the RCS using the two approaches for background subtraction (the dotted line represent the linear fit approach).

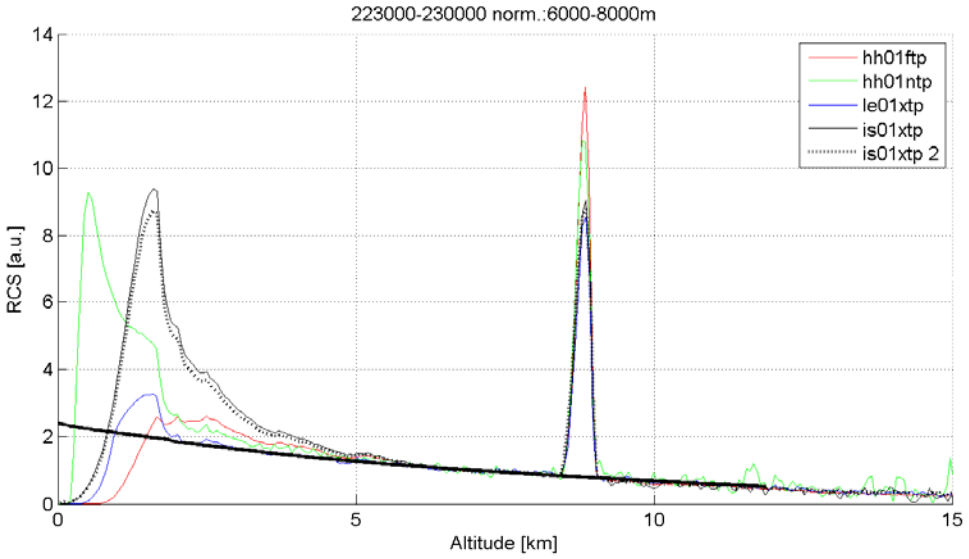

Fig. 35. Same as Figure 82, for night time measurements on 12th of May 2009.

CAML participation within EARLI09 campaign was intended to check the system performance by comparisons with other more sophisticated and well established lidar systems. Thus, for our purpose (comparison of the raw elastic backscatter signal at 532nm, total unpolarized light) the comparisons were possible with the following systems: Martha and PolyXT ("le01" and "le02" from Leipzig), Caeli ("bh01" from Bilthoven) and ARL2 ("hh01" from Hamburg). Note that "bh01" and "hh01" have two receiving telescopes (for near field and far field) and thus the maximum number of signals we compare with is six. The first step in the intercomparison (preliminary results shown during campaign) consists of the comparison of the raw signals (normalized). Figures 34 and 35 show typical behavior of the CAML system during day time and night time operation. While during day time (Fig. 82), the CAML signals compare reasonable well with the others, it is not the case for night time (Fig. 83). Note that for the daily measurements, the Hamburg system (hh01ftp and hh01ntp) had some issues with the photon counting acquisition and thus their signals are not reliable. As seen, the CAML signals increased a lot in the near field (over first ~ 7km). This behavior was systematically observed over all sessions. More details are given in the report provided after the campaign (M. Adam, 2010, private communication). The campaign, through the comparison with the other systems, at the same wavelength, showed that CAML system is unstable. More exactly, the telescope is probably temperature dependent (even if the company said it was not). The possibility of the misalignment is highly probable. Very little defocus, due to the temperature variation, either because the lens is temperature dependent and thus the focal point changes (while the fiber remains in the same position) or the telescope frame is temperature dependent and thus the fiber position changes (while the focal point is the same) results in different overlap functions. A non-accurate overlap correction function results in non-accurate retrievals of backscatter and extinction coefficients.

After system return from Leipzig the system did not perform in a satisfactory way, the signal to noise ratio was too low indicating a misalignment of the system. The first step was to carefully perform the three tests described in the lidar manual in order to estimate the current state of the system and to optimize it. Optical fibers were changed. At the moment, the SNR is not optimal. Unfortunately we could not further improve the signal. The company did not show interest in helping and coming over to perform tests. Within these conditions, we are not confident with the optical properties retrieved. The best one can do with this kind of data is to only consider it for determination of PBL height (Planetary Boundary Layer) or other structures within atmosphere.

First results from the Lidar (CAML) can be found in Barnaba et al., 2010.

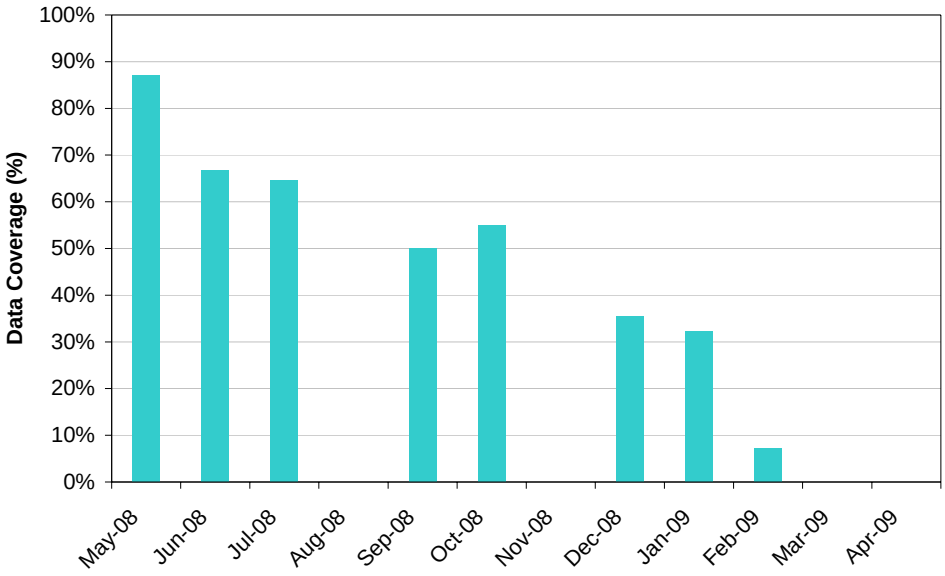

Fig. 36. Data coverage for particle hygroscopic growth measurements during the EUCAARI intensive measurement period

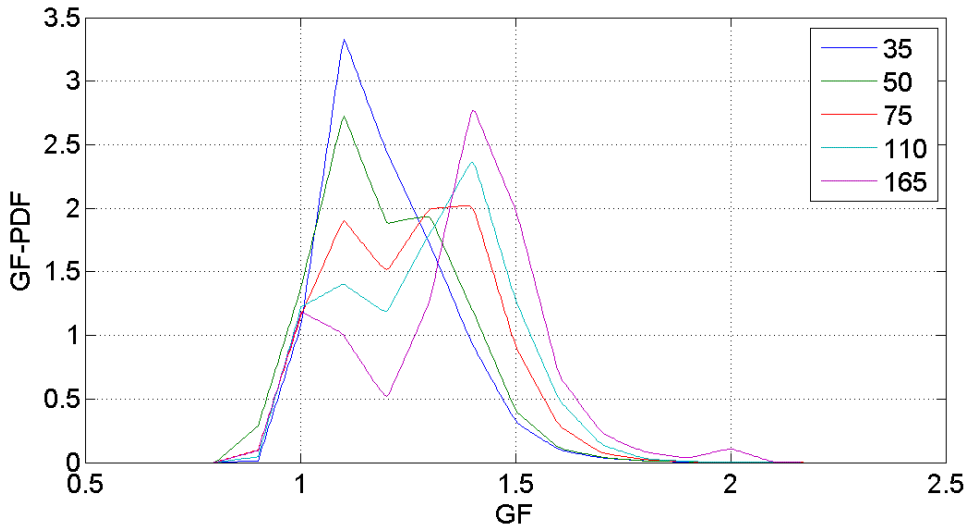

Fig. 37. Probability distribution functions for particle hydroscopic growth factors at 90% RH for 5 dry particle diameters (35 – 165 nm).

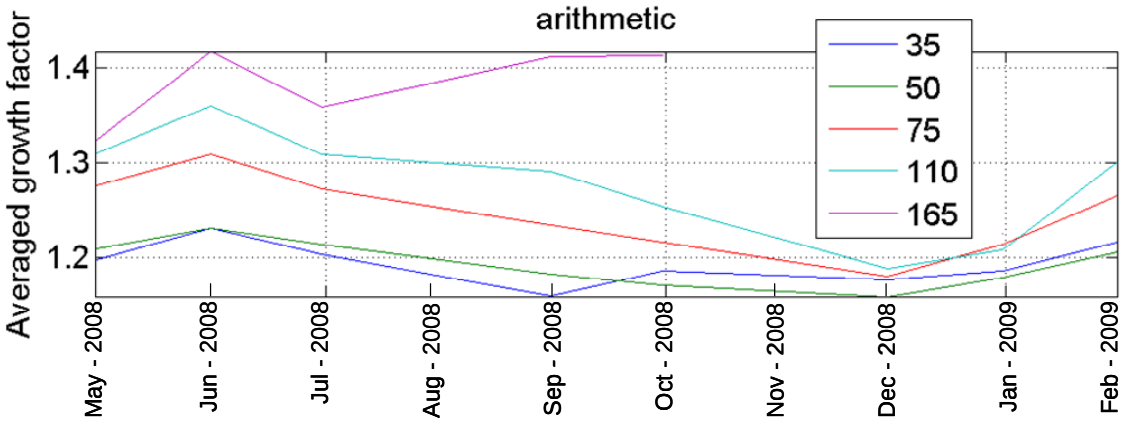

Fig. 38. Monthly average hygroscopic growth factor at 90% RH for 5 dry particle diameters (35 – 165 nm).

H-TDMA measurements

Particle hygroscopic growth measurements at 90% relative humidity (RH) were performed for 122 days during the EUCAARI intensive observation period from May 2008 to February 2009 (33% data coverage), such covering the 4 seasons of a year, in accordance with the EUSAAR measurement program (Fig. 36).

This set-up was not fully following the EUSAAR recommendation: the T-controlled enclosure, the humidification of the aerosol flow up to 90% RH, the measurement of RH in the aerosol flow, and the dew-point measurement in the sheath air flow were missing. However, essential requirements like a feedback between RH measurements and water bath temperature allowed us to keep RH in the range 90±0.25% for 78% of the measuring time, and in the range 90±0.5% for 89% of the time. Selected dry diameters were 35, 50, 75, 110, and 165 nm, following the agreement within EUSAAR. Measurements at 265 nm were not possible because they led too often to arc flashes between the 2 electrodes of DMA2. Measurements at 165 nm were not always available, because the low number of 165 nm dry particles generally led to very noisy hygroscopic growth factor (GF) measurements for this diameter. Data were corrected for the difference in DMA1 and DMA2 sizing using dry scans performed on 23/01/2009, and for difference in RH in DMA2 with respect to the target RH = 90% according to the procedure described by Gysel et al., 2009.

Figure 37 shows the probability distribution function for the growth factor (GF) at 90% RH for 5 particle dry diameters. Three hygroscopic modes can be observed with different probability of occurrence according to particle sizes. A mode at about GF = 1.1 (almost hydrophobic particles) is the most frequent for particle dry diameter = 35 and 50 nm, but is present for all other diameters. A mode at GF = 1.3 – 1.4 (internal mixture of hydrophobic and hydrophilic species) is also observed for all dry diameters, and gets predominant for all dry diameters larger than (or equal to 75 nm). A mode at GF = 2 (very hydrophilic particles, almost comparable to sea salt) is observed for particle dry diameters = 165 nm. These observations are consistent with the current understanding that most small particles (Dp ≤ 50 nm) from primary sources are mainly hydrophobic (like e.g. elemental carbon, EC), and that particle growth results from the accumulation of secondary particulate matter (e.g. NH_4NO_3, $(NH_4)_2SO_4$, water soluble secondary organic aerosol), which is more hygroscopic.

However, GF are on average rather small, which suggests that hydrophobic constituents (probably carbonaceous species) contribute for more than half of the particle volume for Dp ≤ 110 nm. GF increase with particle size is small (Fig. 38), and could probably be explained by the Kelvin effect only. Seasonal variations in mean GF show a maximum in June (intense photochemistry producing secondary aerosol), and minimum in December.

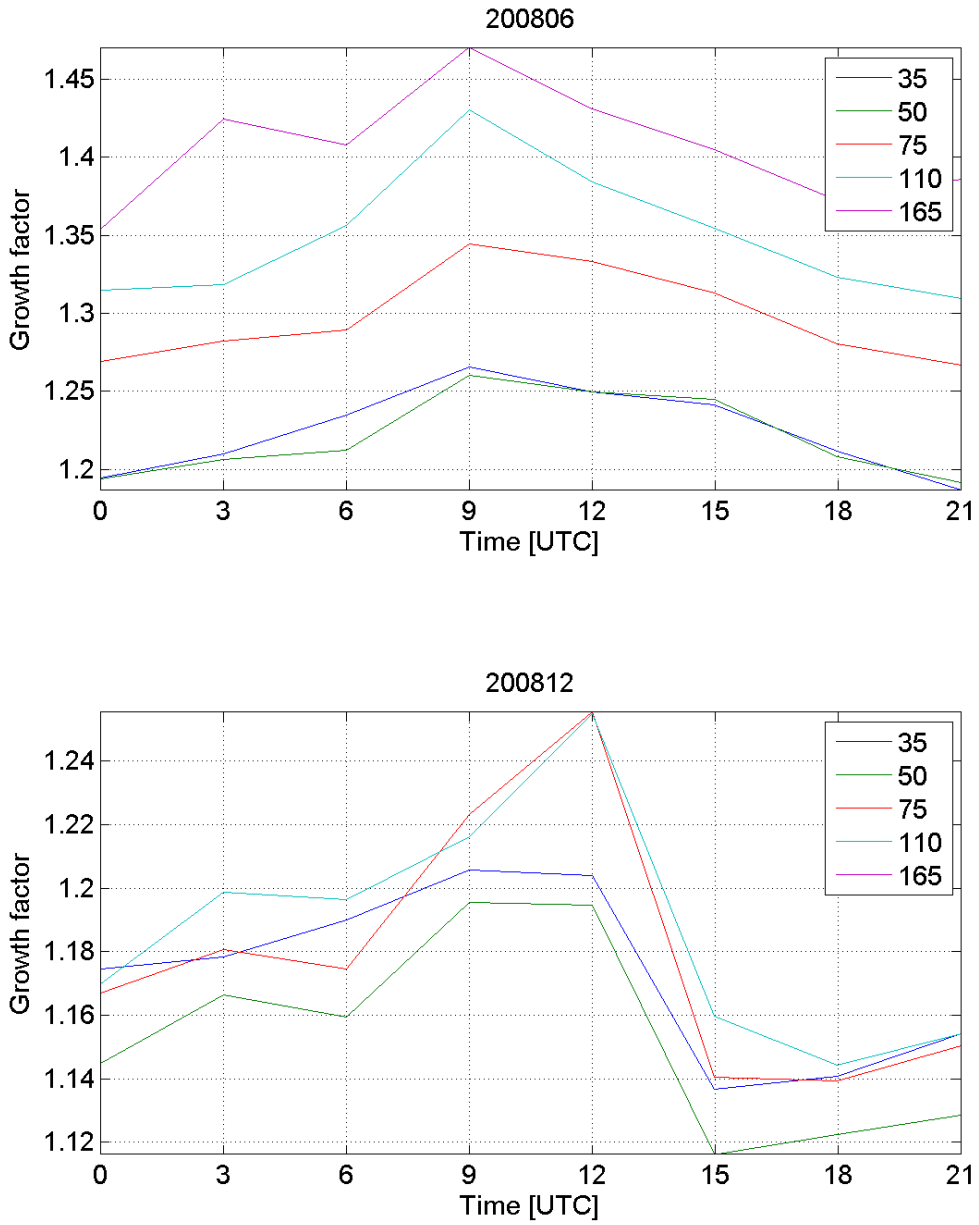

Fig. 39. Diurnal cycles of the hygroscopic growth factor at 90% RH for June (top) and December (bottom) 2008 for 5 dry particle diameters (35 – 165 nm).

Fig. 39 shows that GFs are larger during daytime than during nighttime both in summer and winter. This suggests that the daily evaporation / condensation cycle is dominated by hydrophobic constituents (probably organic species) rather than by NH_4NO_3 (volatilisation of NH_4NO_3 from the particulate phase would indeed lead to a decrease in GF during daytime). The amplitude of the diurnal variations is slightly larger for the largest particles (ca 1.1) than for the smallest ones (ca. 1.05), and independent of the season, although (as already stated), particles are generally more hydrophilic in June than in December.

All H-TDMA data acquired over May 2008 – Feb. 2009 were processed and submitted to the EBAS data base in June 2010.

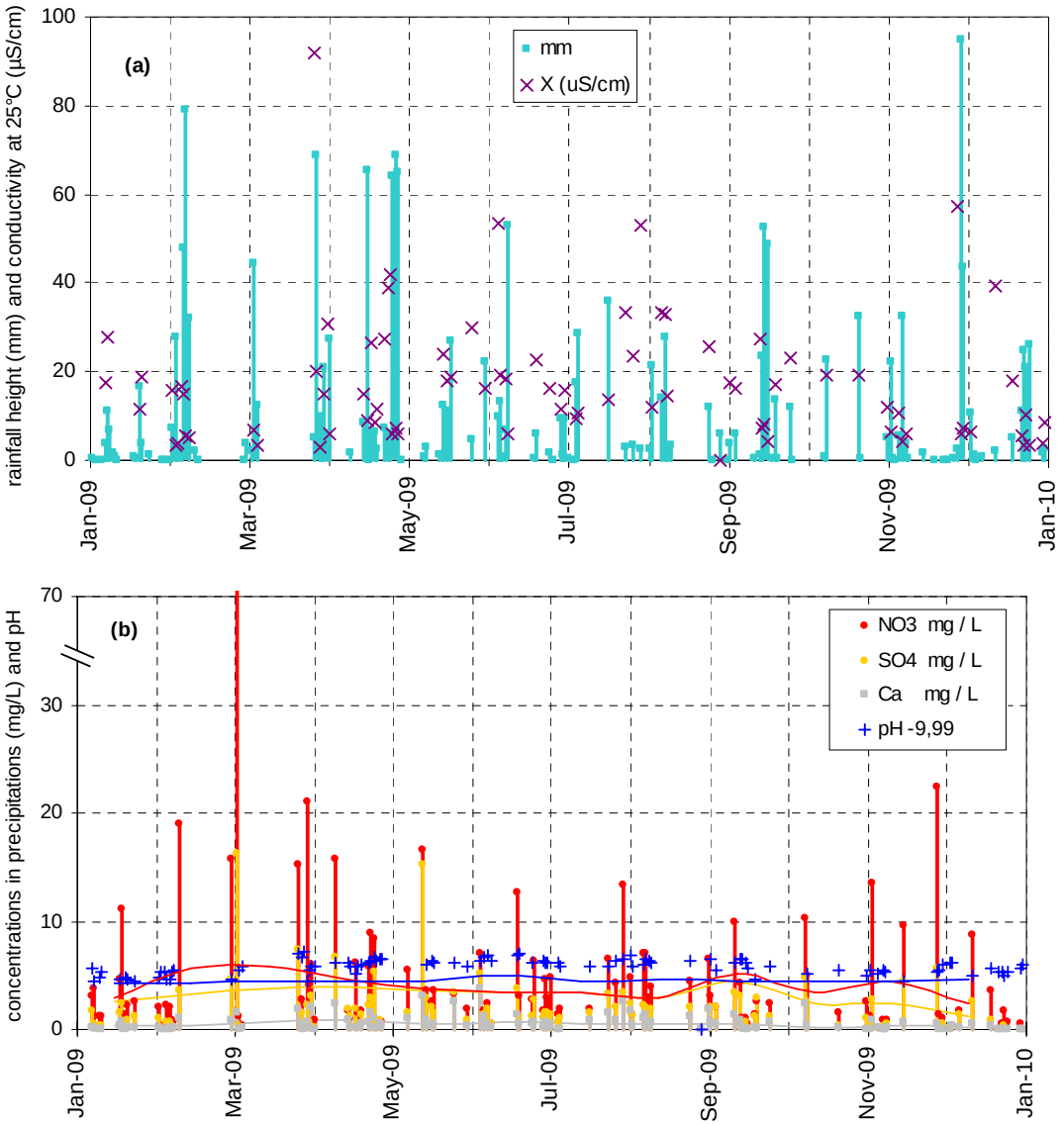

Fig. 40.(a) Precipitation amount, conductivity and (b) concentrations of 3 main precipitation components and pH recorded in 2009 (bars and crosses), and during the 1990-1999 period (lines).

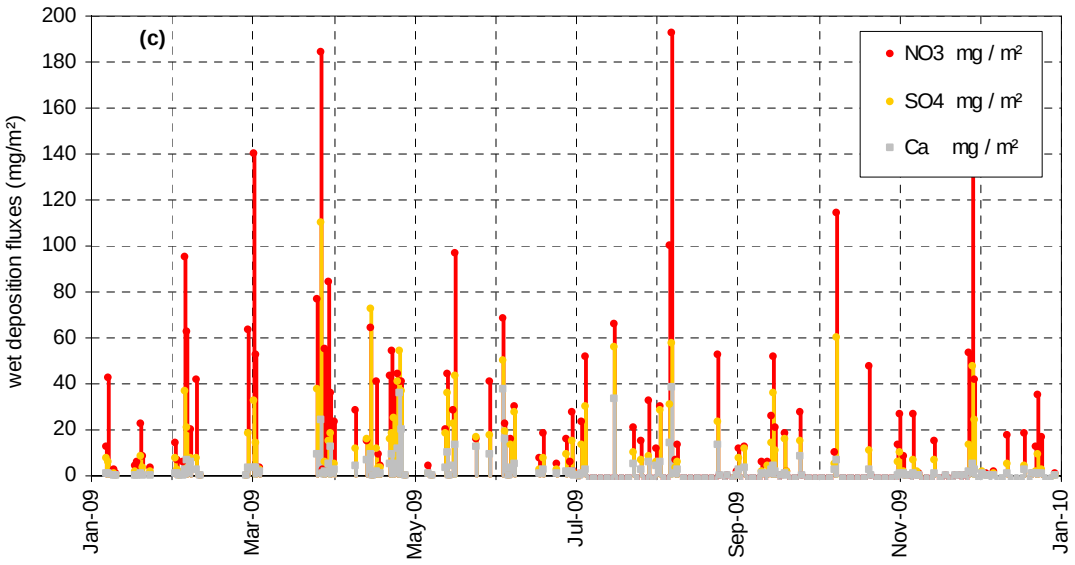

Fig. 41. Wet deposition fluxes of 3 main components in rain water in 2009.

Precipitation chemistry

In 2009, 108 precipitation samples were collected and their ion content determined. The pH-values for 95 and the total conductivity for 81 of those samples were measured, not sufficient water volume was available for the remaining samples. The precipitation height of the collected events ranged from 0.1 to 95 mm (Fig. 40) for a total of 1408 mm (*vs.* 1292 mm collected in 2008 and 879 mm in 2007).

The ranges of concentrations measured in these samples are indicated in Table 4. Volume weighted mean concentrations of all species but Na^+ were in 2009 smaller than the 1990-1999 averages. The precipitation samples collected in 2009 were all acidic, except two.

Wet deposition occurred rather evenly from mid February till mid December (Fig. 40). The annual wet deposition flux of the main acidifying and eutrophying species were 1.6, 3.4, and 1.4 g m^{-2} for SO_4^{2-}, NO_3^-, and NH_4^+, respectively. These fluxes were slightly larger than in 2008 with values of 1.5, 3.0 and 1.2 g m^{-2} for the respective species (see also Fig. 41 for wet deposition fluxes).

Table 4. Statistics relative to the precipitation samples collected in 2009 (averages are volume weighted)

	pH	cond.	Cl^-	NO_3^-	SO_4^{2-}	Na^+	NH_4^+	K^+	Mg^{2+}	Ca^{2+}
		µS cm^{-1}	mg l^{-1}	mg l^{-1}	mg l^{-1}	mg l^{-1}	mg l^{-1}	mg l^{-1}	mg l^{-1}	mg l^{-1}
Average	5.38	12.98	0.26	2.25	1.04	0.33	0.92	0.05	0.05	0.34
Min	4.41	2.83	0.01	0.04	0.04	0.02	0.00	0.00	0.00	0.02
Max	7.10	91.7	12.5	70.0	16.2	6.6	21.5	1.1	0.9	3.8
1990-1999	4.4	24.86	0.44	3.94	3.07	0.23	1.25	0.09	0.06	0.45

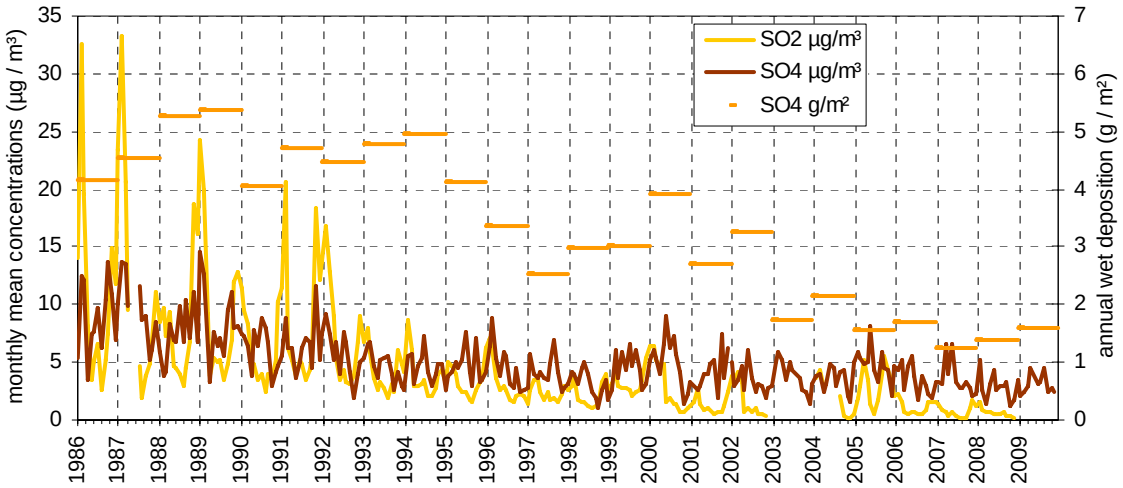

Fig. 42. Oxidized sulfur species monthly mean concentrations and yearly wet deposition.

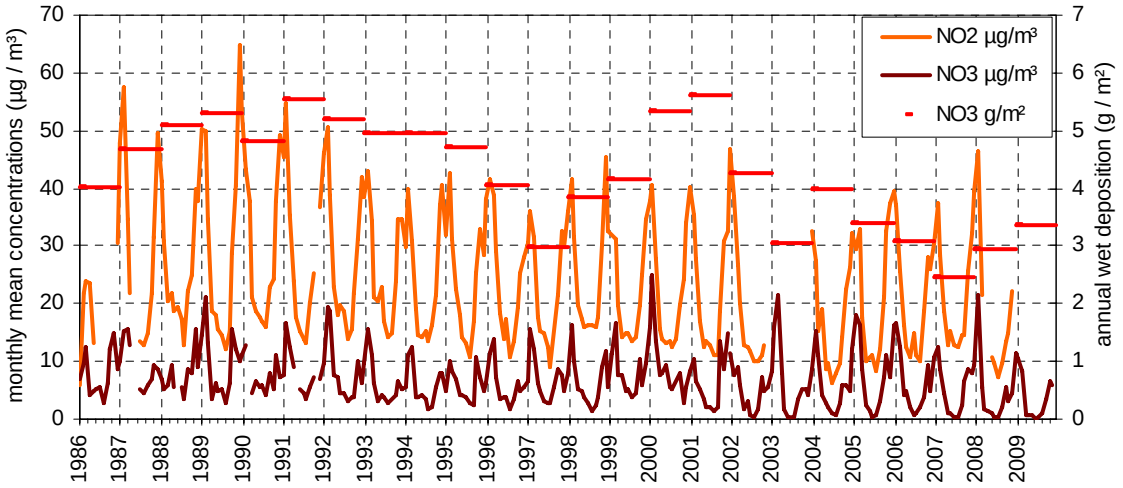

Fig. 43. Oxidized nitrogen species monthly mean concentrations and yearly wet deposition.

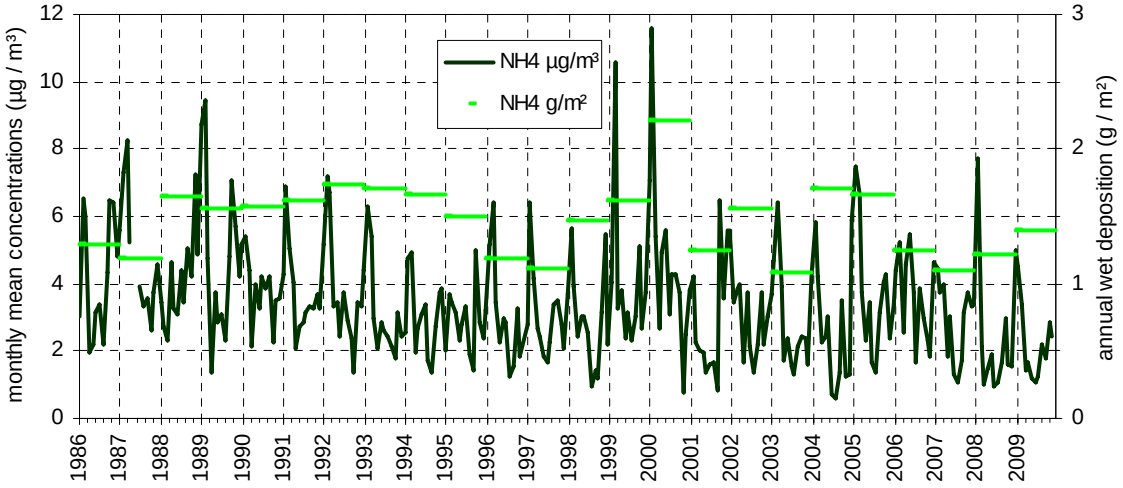

Fig. 44. Reduced nitrogen species monthly mean concentration and yearly wet deposition.

Results of year 2009 in relation to more than 2 decades of monitoring activities

Sulfur and nitrogen compounds

Particulate SO_4^{2-} showed a clear decreasing trend from 1986 to 1998 (a factor of about 3), but seems to stabilize around the mean value for the 90's since then (see Fig. 42). Both winter maxima and summer minima monthly mean concentrations of sulfur dioxide (SO_2) decreased by a factor of more than 5 over the past 24 years (Fig. 42). These data show that locally produced SO_2 decreased much more than possibly long-range transported SO_4^{2-} over the past 20 years. It should be kept in mind that SO_4^{2-} concentrations were measured in PM10 or in PM2.5 from 2002 onwards, whereas it was measured in TSP (Total Suspended Particulate) from 1986 to 2001. However, simultaneous sampling of PM10 and TSP over 14 months showed that SO_4^{2-} in PM10 is generally less than 5 % lower than in TSP. It should also be mentioned that SO_4^{2-} is mainly present in the PM2.5 fraction (see Fig. 21). From 2005 onwards the calculations were as following SO_4^{2-}(PM10) = SO_4^{2-}(PM2.5) x <SO_4^{2-}(PM10)/ SO_4^{2-}(PM2.5))> (the average <SO_4^{2-}(PM10)/ SO_4^{2-}(PM2.5))> is calculated based on the 4-6 simultaneous PM10 and PM2.5 samples collected each month. SO_4^{2-} wet deposition in 2009 was among the lowest values recorded.

Monthly mean concentrations of nitrogen dioxide (NO_2) do not show such a pronounced decreasing trend over the last 2 decades (Fig. 43) as seen for SO_2. Wintertime NO_2 maxima indeed remained quite constant over 1993-2002, and did not reflect the 30 % abatement in NO_x emissions reported for the 1992-2000 period (Perrino and Putaud, 2003). Particulate NO_3^- annual mean concentration observed in 2003 - 2009 were comparable to values observed in the mid-90's, mainly due to high wintertime values. It should be noted that since October 2000, NH_4 and NO_3^- have been measured mostly from quartz fibre filters, which are known to lose NH_4NO_3 at temperatures > 20 °C. This might contribute significantly to the fact that NO_3^- summertime minima are particularly low since 2001. Furthermore, NO_3^- was measured from PM10 or in PM 2.5 from 2002, and no more from TSP, as over the 1986 to 2001 period. However, simultaneous sampling of PM10 and TSP over 14 months showed that NO_3^- in PM10 is generally less than 5 % lower than in TSP, like SO_4^{2-}. From 2005 and onwards the calculations were as following NO_3^- (PM10) = NO_3^-(PM2.5) x < NO_3^-(PM10)/ NO_3^-(PM2.5))> (the average < NO_3^-(PM10)/ NO_3^-(PM2.5))> is calculated based on the 4-6 simultaneous PM10 and PM2.5 samples collected each month. NO_3^- wet deposition annual flux observed in 2009 was rather low compared to the last 2 decades recorded in Ispra.

Monthly mean concentrations of NH_4^+ in the particulate phase appear to decrease slightly over 1986 – 2009 (Fig. 44), especially because summertime minima decreased. There is no clear trend

regarding NH_4^+ wintertime maxima, especially this winter saw rather high values. On average, NH_4^+ can neutralize > 98 % of the acidity associated with NO_3^- and SO_4^{2-} in the particulate phase (see Fig. 18). NH_4^+ is also quite well correlated with $NO_3^- + SO_4^{2-}$ in rainwater.

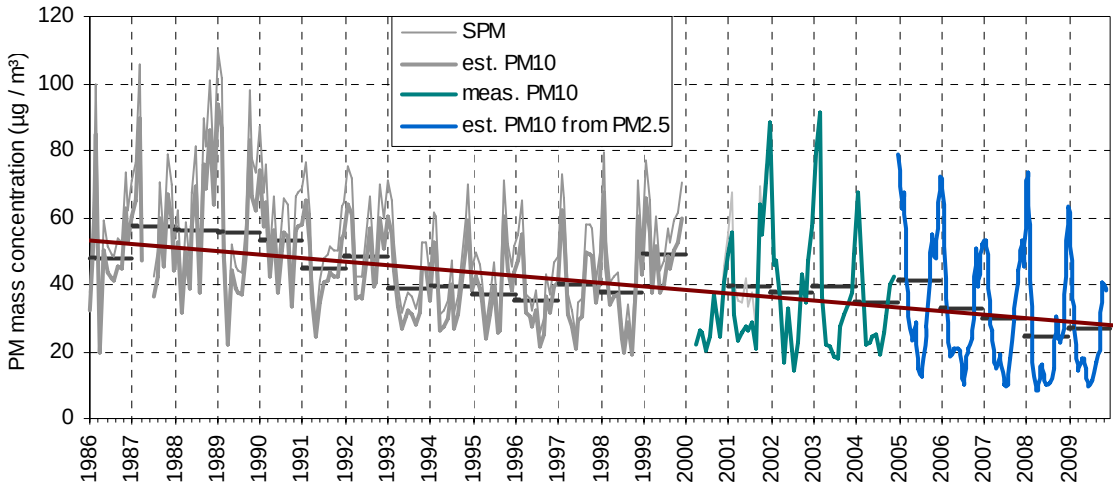

Fig. 45. Particulate matter mass concentration monthly and annual averages. The black lines are the annual PM10 average and the dark red line is the annual trend. All values in the figure are from gravimetric measurements or values estimated from gravimetric measurements.

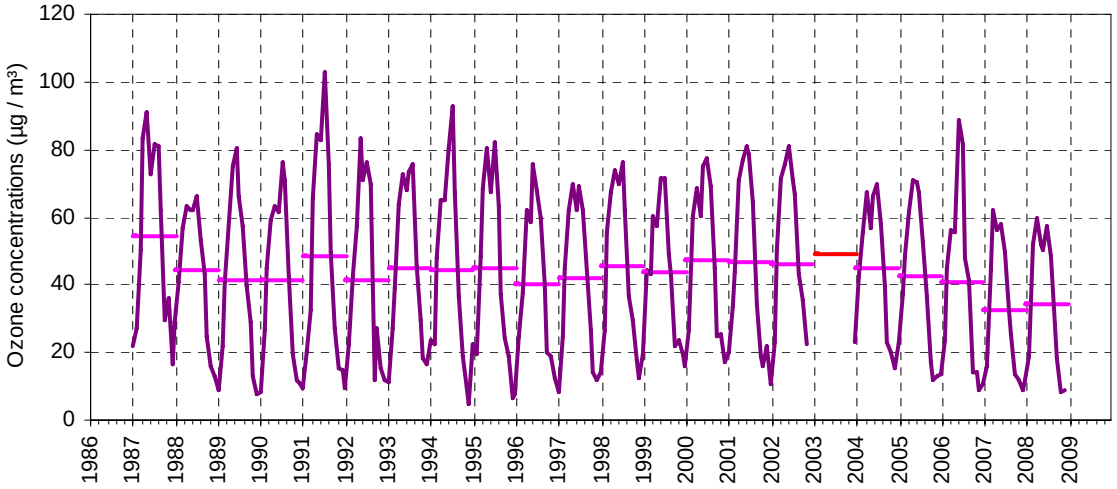

Fig. 46. Ozone yearly and monthly mean concentrations at JRC-Ispra. 2003 data from Malpensa airport (Source: ARPA Lombardia).

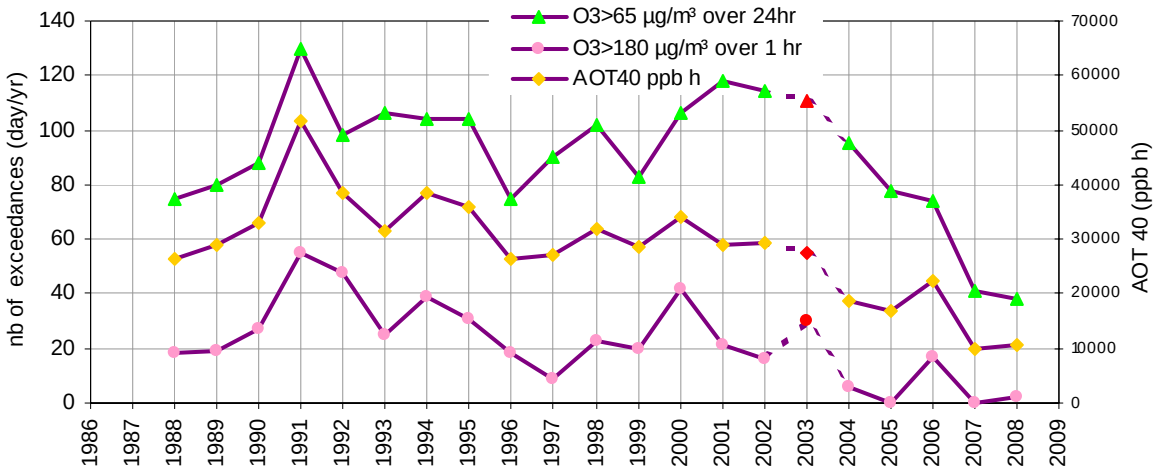

Fig. 47. AOT40 values and number of days on which indicated O3 limit values were reached. Red symbols indicate estimates based on Malpensa airport data (no data from Ispra in 2003, see also Fig. 46 for additional information).

NH_4^+ annual wet deposition was rather similar to the last 2 decades recorded in Ispra. It should be mentioned that from the year 2002 NH_4^+ was measured in the PM10 or in the PM2.5 fraction (from 2005 and onwards the calculations were as following NH_4^+(PM10) = NH_4^+(PM2.5) x < NH_4^+(PM10)/ NH_4^+(PM2.5))> (the average < NH_4^+ (PM10)/ NH_4^+(PM2.5))> is calculated based on the 4-6 simultaneous PM10 and PM2.5 samples collected each month.)

Finally, it should be mentioned that for the 2009 yearly averages for particulate SO4, NO3, and NH4 in PM10 (estimates) were the lowest ever recorded at the Station (2.5, 3.4, and 1.8 µg/m³, respectively).

Particulate matter mass

The PM10 values observed in 2009 agree with the general decreasing trend in PM10 observed over the last 2 decades (Fig. 45). In fact, the annual average PM10 concentration reached a historic minimums of 24.6 µg/m³ in 2008 (26.8 µg/m³ in 2009) since the measurements were started in 1986. A linear fit indicates that PM10 has been decreasing by about 0.9 µg m^{-3} yr^{-1} during 1986-2009. It should be kept in mind that PM10 concentrations were estimated from TSP mass concentration measurements (carried out by weighing at 60 % RH and 20 °C cellulose acetate filters sampled without any particle size cut-off and "dried" at 60 °C before and after sampling) over 1986-2000, based on a comparison between TSP and PM10 over the Oct. 2000 - Dec. 2001 period (R^2 = 0.93, slope = 0.85). In addition, from the years 2005-2009 measured PM2.5 values were converted into PM10 values.

It should be mentioned that the European directive 1999/30/EC states that the 24-hr EU PM10 limit value of 50 µg/m³ should not to be exceeded more than 35 times a calendar year from 1st of January 2005 onwards (EN 12341 method using weighing of filters at 50 % RH.), and that the annual EU PM10 limit value should be below 40 µg/m³ from 1st of January 2005 onwards. In addition, the European directive 2008/50/EC states that the annual EU PM2.5 limit value should be below 25 µg/m³ from 1st of January 2015 onwards (EN 14907 method using weighing of filters at 50 % RH.).

Ozone

Figure 46 shows monthly and yearly mean O_3 concentrations observed since 1987. It should be mentioned that ozone was not measured in 2009 (but restarted in Jan. 2010) and that there were an acquisition breakdown in 2003. To close the gap in 2003, O_3 data from Malpensa airport have been used to estimate values based on a comparison between Ispra and Malpensa during 2004. No clear trend in O_3 annual mean concentrations can be deduced from the observations over 1987-2008, but a small decreasing trend may be significant over 2000-2008. E.g. the annual average in 2007 and 2008

were the lowest measured since 1986. In addition, the summertime monthly maximums in 2007 and 2008 were actually the two lowest recorded.

Figure 47 shows that AOT40 (Accumulated Ozone exposure over a Threshold of 40 ppb), the vegetation exposure to above the O_3 threshold of 40 ppb (about 80 µg/m³) started to decrease again from 2002. This trend continued in 2008 with a very low value of 10800 ppb h. Also the number of days with a mean O_3 concentration > 65 µg/m³ (vegetation protection limit) have a new historic minimum of 38 days only. The number of days on which the limit value for public information (180 µg/m³ over 1hr) was reached or exceeded also decreased from 2000 (2003 and 2006 are exceptions due to heat waves). In 2008 this limit has been exceeded on two days only (see also Gruening et al., 2009).

Conclusions

Meteorological data were acquired directly at the EMEP site during 2009 using the Vaisala WXT510 weather transmitter.

The gas phase measurements were not measured during the year 2009, due to lack of man-power, but all of the gas phase measurements have been restarted in January 2010.

Aerosol sampling on quartz fibre filter for gravimetric and chemical analyses were also performed over the whole year. We collected PM2.5 daily and PM10 four times a month with two respective Partisol samplers. All PM2.5 samples were analyzed for carbonaceous components with the new Sunset Lab OC/EC instrument using the EUSAAR-2 protocol. The ionic balance in both rainwater and aerosol samples demonstrate a perfect agreement between NH_4^+ measurement on the one hand, and NO_3^- + SO_4^{2-} measurements on the other hand. Particle number size distributions were performed with a DMPS and an APS along the year, except for maintenance periods. The average aerosol density of 1.37 g/cm^3, derived from the gravimetric mass and DMPS plus APS volume was still a bit low, especially compared to the 2005 value of 1.5 g/cm^3. Aerosol scattering and absorption coefficients were derived from Nephelometer and Aethalometer measurements, applying state-of-the-art corrections to these measurements. However, these data were not normalized to a standard relative humidity. The extinction-to-mass ratio of 4.5 m^2 g^{-1} measured in 2009 is comparable to 4.7 m^2 g^{-1} obtained in 2008. It is consistent with the value that can be calculated from the mean PM2.5 chemical composition, which sums up to 4.4 m^2 g^{-1} in 2009 (see Table 3).

The 2009 data listed by EMEP as core parameters have been reported to Chemical Co-ordinating Centre of EMEP.

With the assumption used to estimate POM and dust from organic carbon (OC) and Ca^{2+}, respectively, the whole PM2.5 mass concentration could be explained rather well in 2009 except for a few occasions. $PM_{2.5}$ average chemical composition was dominated by carbonaceous species (POM: 47%, EC: 8%), followed by secondary inorganics (NH_4^+:9%, NO_3^-: 10%, SO_4^{2-}: 18%). The contribution of sea-salt ions and mineral dust were about 2%. However, there is a clear increase of the NO_3^- contribution when shifting from cleaner (PM2.5 < 15 µg/m³) to more polluted periods (PM2.5 > 25 µg/m³). The PM10 mass annual average of 26.8 µg/m³ did not exceed the EU annual limit value (40 µg/m³). The long term time series still suggests a PM10 mass concentration decrease of 0.9 µg m^{-3} yr^{-1} over the last more than 2 decades (about 25 years of records). It should be mentioned that the two lowest PM10 values since 1986 were measured in 2008 and 2009.

Average particle number in 2009 was about 7400 cm^{-3} (range 1200 – 18300 cm^{-3}) Particle number size distributions were generally slightly bimodal, with a submicron mode at ca. 100 nm (dry) and a less pronounced coarse mode around 2 μm. The particle mean geometric diameter ranged 35 – 120 nm (maximum values observed in winter). Seasonal variations in particle hygroscopic growth were measured for the first time in Ispra over April 2008 – March 2009. Growth factor at 90% RH are minimum in December (<1.2) and range between 1.25 and 1.35 (for particle dry diameter ranging from 35 to 110 nm) in June. Atmospheric aerosol scattering and absorption coefficients at various wavelengths were derived from Nephelometer and Aethalometer measurements at not controlled (but generally lower than ambient) relative humidity. The mean single scattering albedo at λ = 550 nm (at RH generally < 40 %) was 0.76 in 2009.

The aerosol extensive variables measured at JRC-Ispra (at ground level) all follow a comparable seasonal trend with minima in summer. These variables are generally well correlated and lead to reasonable degrees of chemical, physical, and optical closures.

Aerosol backscatter and extinction profiles were obtained with a LIDAR in Jan.-April and Oct.-Nov. during 2009. Due to instrumental problems and meteorological conditions, only 38 out of 157 profiles could be submitted to the EARLINET database.

The concentrations of all rainwater components (Cl^-, NO_3^-, SO_4^{2-}, NH_4^+, K^+, Mg^{2+}, and Ca^{2+}) but Na^+ were all lower in 2009 compared to the 1990-1999 average. The annual wet deposition flux of the main acidifying and eutrophying species were 1.6, 3.4, and 1.4 g m^{-2} for SO_4^{2-}, NO_3^-, and NH_4^+, respectively. These fluxes were slightly larger than in 2008 but well below the last decade's averages.

References

Anderson, T.L., and Ogren, J.A., Determining aerosol radiative properties using the TSI3563 integrating nephelometer, *Aerosol Sci. Technol.*, **29**, 57-69, 1998.

Arnott, W.P., Hamasha, K., Moosmüller, H., Sheridan, P.J., and Ogren, J.A., Towards aerosol light-absorption measurements with a 7-wavelength Aethalometer: Evaluation with a photoacoustic instrument and a 3 wavelength nephelometer., *Aerosol Sci. Technol.*, **39**, 17-29, 2005.

Barnaba, F., Putaud, J.P., Gruening, C., Dell'Acqua, A., Dos Santos, S., Co-located in-situ, total-column and height-resolved aerosol observations: Implications for ground-level PM estimation from remote sensing. *J. Geophys. Res.*, **115**, D10204, doi:10.1029/2009JD012451, 2010.

Burch, D. E.; Gates, F. J.; Pembrook, J. D., Ambient carbon monoxide monitor. Research Triangle Park, NC: U.S. Environmental Protection Agency, Environmental Sciences Research Laboratory; report no. EPA-600/2-76-210, 1976.

Cavalli, F., Putaud, J.P., Toward a standardised thermal-optical protocol for measuring atmospheric organic and elemental carbon: the EUSAAR protocol, *Atmos. Meas. Tech.*, **3**, 79-89, 2010.

Cooke, W.F., Liousse, C., Cachier, H., and Feichter, J., Construction of a 1x1°fossil fuel emission data set for carbonaceous aerosol and implementation and radiative impact in the ECHAM4 model, *J Geophys. Res.*, **104**; 22,137-22, 1999.

Dell'Acqua, A., Putaud J.P., Gruening, C., Study of the JRC-Ispra EMEP site representativeness for short-lived atmospheric species measurements, *JRC report* EUR 24312 EN, 2010.

EMEP manual for sampling and chemical analysis (1995). *EMEP/CCC-Report 1/95.* (*Revised 1996; 2001; 2002).* 1995.

European Directive 1999/30/EC. Relating to limit values for sulphur dioxide, nitrogen dioxide and oxides of nitrogen, particulate matter and lead in the ambient air. 1999.

European Directive 2008/50/EC. On ambient air quality and cleaner air for Europe. 2008.

Gruening, C., Adam, M., Cavalli, F., Dell'Acqua, A., Martins Dos Santos, S., Pagliari, V., Roux, D., Putaud J.P., Gruening, C., JRC Ispra EMEP – GAW regional station for atmospheric research. 2008 report. *JRC report* EUR 24088 EN, 2009.

Hess, M., Koepke, P. Schult, I., Optical Properties of Aerosols and Clouds: The Software Package OPAC, *Bull. of Am. Meteorol. Soc.*, **79**; 831-844, 1998.

Kiehl, J. T., Schneider, T. L., Rasch, P. J., Barth, M. C., Wong, J., Radiative forcing due to sulfate aerosols from simulations with the National Center for Atmospheric Research Community Climate Model, Version 3 (Paper 1999JD900495), *J. Geophys. Res.,* **105**; 1441-1458, 2000.

McMurry, P., Wang, X., Park, K., and Ehara, K. The relationship between mass and mobility for atmospheric particles: A new technique for measuring particle density, *Aerosol Sci. Tech*., **36**, 227–238, 2002.

Mira-Salama, D., Van Dingenen, R., Gruening, C., Putaud, J.-P, Cavalli, F., Cavalli, P., Erdmann, N., Dell'Acqua, A., Dos Santos, S., Hjorth, J., Raes, F., Jensen, N.R.
Using Föhn conditions to characterize urban and regional sources of particles, *Atmospheric Research* **90**, 159–16, 2008.

Nessler, R., Weingartner, E., and Baltensperger, U., Adaptation of dry nephelometer measurements to ambient conditions at the Jungfraujoch, *Environ. Sci. Technol.*, **39** (7), 2219-2228, 2005.

Petzold, A., H., Schönlinner, M., Multi-angle absorption photometry - A new method for the measurement of aerosol light absorption and atmospheric black carbon, *Journal of Aerosol Science*, **35** (4), 421-441, 2004.

Perrino, C., and Putaud, J.P., Assessment of the EMEP measurement and modelling work in Europe from 1977 until Today: national contribution of Italy, *EUR* 20979 EN, 2003.

Putaud, J.-P., et al. (21 authors), 2004, A European aerosol phenomenology—2: chemical characteristics of particulate matter at kerbside, urban, rural and background sites in Europe. *Atmospheric Environment*, **38**, 2579-2595.

Putaud, J.-P., et al. (39 authors), 2010, A European aerosol phenomenology—3: Physical and chemical characteristics of particulate matter from 60 rural, urban, and kerbside sites across Europe. *Atmospheric Environment*, **44**, 1308-1320.

Rembges, D., Brun, C., Duane, M., Fantechi, G., Geiss, O., Larsen, B., Putaud, J.-P. JRC – Ispra air monitoring station 2000-2001 report. *JRC report* EUR 20998 EN, 2003.

Russell, L.M.: Aerosol organic-mass-to-organic carbon ratio measurements, *Environ. Sci. Technol.*, **37**, 2982-2987, 2003.

Schmid, O., et al., Spectral light absorption by ambient aerosols influenced by biomass burning in the Amazon Basin I: comparison and field calibration of absorption measurements techniques, *Atmos. Chem. Phys.*, **6**, 3443-3462, 2006.

Stratmann, F., Wiedensohler, A. A new data inversion algoritm for DMPS-measurements. *J. Aerosol Sci.*, **27** (Suppl 1), 339-340.

Van Dingenen, R., et al. (28 authors), 2004, A European aerosol phenomenology –1: Physical characterization of particulate matter at kerbside, urban, rural and background sites in Europe, *Atmospheric Environment*, **38**, 2561-2577.

Weingartner, E., Saathoff, H., Schnaiter, M., Streit, N., Bitnar, B., and Baltensperger, U., Absorption of light by soot particles: determination of the absorption coefficient by means of aethalometers, *J. Aerosol Sci.*, **34**, 1445-1463, 2003.

Weitkamp, C. (editor), LIDAR Range-Resolved Optical Remote Sensing of the Atmosphere, *Springer*, New York, 2005.

Links

ARPA Lombardia, http://ita.arpalombardia.it/ITA/qaria/doc_RichiestaDati.asp

Calipso, http://www.nasa.gov/mission_pages/calipso/main/

Chemical Co-ordinating Centre of EMEP, http://www.nilu.no/projects/ccc/.

CLRTAP, http://www.unece.org/env/lrtap/welcome.html

EMEP, http://www.emep.int/

EMEP emission inventory 2000, http://webdab1.umweltbundesamt.at/scaled_country_year.html?cgiproxy _skip=1

Global Atmosphere Watch (GAW), http://www.wmo.int/pages/prog/arep/gaw/gaw_home_en.html

WDCA, http://www.gaw-wdca.org/

World Meteorological Organization (WMO), http://www.wmo.int/pages/index_en.html.

European Commission

EUR 24678 EN– Joint Research Centre – Institute for Environment and Sustainability
Title: JRC Ispra EMEP – GAW regional station for atmospheric research, 2009 report
Author(s): Niels R. Jensen, Carsten Gruening, Mariana Adam, Fabrizia Cavalli, Paolo Cavalli, Fabrizio Grassi, Alessandro Dell'Acqua, Sebastiao Martins Dos Santos, David Roux, Jean-Philippe Putaud
Luxembourg: Publications Office of the European Union
2010 – 69 pp – 21 x 29.7 cm
EUR – Scientific and Technical Research series – ISSN 1018-5593
ISBN 978-92-79-18978-4
doi:10.2788/97714

Abstract

The aim of the JRC-Ispra station for atmospheric research (45°49'N, 8°38'E) is to monitor atmospheric parameters (pollutant concentrations and fluxes, atmospheric particle chemical composition, number size distribution and optical properties) to contribute in assessing the impact of European policies on air pollution and climate change. The station has been operated continuously since November 1985, with a gap in gas phase data in 2003 and 2009 due to a breakdown of the data acquisition system and lack of man-power, respectively.

The measurements performed in 2009 led to annual average of 26.8 and 19 µg m^{-3} for PM_{10} and $PM_{2.5}$, respectively, well below the European annual limit values of 40 µg/m³ (the European directive 1999/30/EC for the year 2005 and onwards) and 25 µg/m³ (European directive 2008/50/EC for the year 2015 and onwards). Carbonaceous species (organic matter plus elemental carbon) are the main constituents of PM2.5 (~57 %) followed by $(NH_4)_2SO_4$ (24 %) and NH_4NO_3 (12 %). The data from 2009 confirmed the seasonal variations observed over the previous years, mainly driven by meteorology rather than by changes in emissions, as revealed by the lidar measurements. Aerosol physical and optical properties were also measured in 2009. The average particle number (from 10 nm to 10 µm) was about 7400 cm^{-3} and the mean geometric diameter was 70 nm. Their hygroscopic growth at 90% RH varies from <1.2 in December to 1.25 – 1.35 (size dependent) in June. The mean (close to dry) aerosol single scattering albedo at λ = 550 nm was 0.76, i.e. low compared to the values generally observed in Europe, which means that the cooling effect of aerosols is reduced in our region compared to others.

Long-term trends (over > 20 years) show consistent decreases in sulfur concentrations and deposition, PM mass concentration (about -0.9 µg m^{-3} yr^{-1}), and from 2003 onwards also a slight decease in ozone concentrations too. The decreasing trends in oxidised and reduced nitrogen species are much less pronounced.

How to obtain EU publications

Our priced publications are available from EU Bookshop (http://bookshop.europa.eu), where you can place an order with the sales agent of your choice.

The Publications Office has a worldwide network of sales agents. You can obtain their contact details by sending a fax to (352) 29 29-42758.

The mission of the JRC is to provide customer-driven scientific and technical support for the conception, development, implementation and monitoring of EU policies. As a service of the European Commission, the JRC functions as a reference centre of science and technology for the Union. Close to the policy-making process, it serves the common interest of the Member States, while being independent of special interests, whether private or national.

LB-NA-24678-EN-C